Published for SISSA by Springer

Received: February 25, 2025
Accepted: May 16, 2025
Published: June 25, 2025

Bounds on variations of the strange quark mass from Big Bang nucleosynthesis

Ulf-G. Meißner[a,b,c] **Bernard Metsch**[b,a] **and Helen Meyer**[a]

[a] *Helmholtz-Institut für Strahlen- und Kernphysik and Bethe Center for Theoretical Physics, Universität Bonn, D-53115 Bonn, Germany*
[b] *Institute for Advanced Simulation (IAS-4), Forschungszentrum Jülich, D-52425 Jülich, Germany*
[c] *Peng Huanwu Collaborative Center for Research and Education, International Institute for Interdisciplinary and Frontiers, Beihang University, Beijing 100191, China*

E-mail: meissner@hiskp.uni-bonn.de, metsch@hiskp.uni-bonn.de, hmeyer@hiskp.uni-bonn.de

Abstract: We analyze the effect of a variation of the strange nucleon matrix element $\langle N|m_s\bar{s}s|N\rangle$ on the abundances of the light elements produced in the Big Bang. For that, we vary the nucleon mass in the leading eight reactions that involve neutrons, protons and the four lightest nuclei. We use various available Big Bang nucleosynthesis codes and find that the measured deuterium and ^{4}He abundances set strict limits on the nucleon mass variations. This translates into an upper bound of possible variations of the strange quark mass, $|\Delta m_s/m_s| \leq 5.1\%$.

Keywords: Quark Masses, Early Universe Particle Physics, Effective Field Theories, Hadronic Spectroscopy, Structure and Interactions

ArXiv ePrint: 2502.15409

Open Access, © The Authors.
Article funded by SCOAP^3.

https://doi.org/10.1007/JHEP06(2025)244

JHEP06(2025)244

Contents

1 Introduction

Big Bang nucleosynthesis (BBN) is a fine laboratory for studying possible variations of the fundamental constants of nature as well as to search for new physics effects, see e.g. [1–11]. Here, we will consider the first issue, namely the bounds on variations of certain parameters from the primordial element abundances. Mostly, one has studied the variation of the electromagnetic fine-structure constant $\alpha_{\rm EM}$ (for a recent work with many references, see [12]) or of the light quark masses m_u, m_d (or alternatively, the Higgs vacuum expectation value (VEV) v), for very recent works see refs. [13, 14].

However, the nucleon and thus the nuclei contain a certain amount of strangeness as indicated by the non-vanishing matrix elements $\langle N|m_s\bar{s}s|N\rangle$ or $\langle N|m_s\bar{s}\gamma_\mu s|N\rangle$, just to mention two [15, 16]. Since the nuclei that take part in the BBN reaction network are made of neutrons and protons, their masses are also sensitive to the amount of strangeness in the nucleon and similarly, the mass differences of the pertinent reactions depend on the precise value of the matrix-element $\langle N|m_s\bar{s}s|N\rangle$. Such effects have not been considered before. Note that we are not talking about hypernuclei here, which are nuclei that contain one or two hyperons.

There are many other possible sources of strangeness in the BBN reaction network. First, kaon loops could influence the vector coupling constant that plays a role in neutron β-decay. Such effects have been shown to be tiny [17] and can thus be neglected. Further, in the boson-exchange models of the nuclear force that underlie the modeling of atomic nuclei, strangeness could enter via η-exchanges or πK, KK loops. While the η coupling to the nucleon is very small and such effects can be neglected, see e.g. [18] and references therein, loops involving kaons are of such short distance, that they can effectively be absorbed in the

JHEP06(2025)244

four-nucleon contact interactions that are used in the modern theory of nuclear forces [19]. As it turns out, the dominant strangeness effect in BBN is due to the mass shift $\langle N|m_s\bar{s}s|N\rangle$, which enters the nucleon mass via the trace anomaly of the energy-momentum tensor. As will be shown below, this matrix element is of the order of 50 MeV, and such a mass shift can strongly influence the BBN network.

The manuscript is organized as follows. In section 2 we discuss the determination of the matrix element $\langle N|m_s\bar{s}s|N\rangle$ and give the bounds on its value. Section 3 contains the details of the calculational procedure. First, we consider the nucleon mass dependence of nuclear quantities like binding energies and scattering parameters, making use of the results from pionless EFT as well as Nuclear Lattice EFT (NLEFT). Second, we discuss the modeling of the nucleon mass dependence of nuclear reaction rates, in particular of the leading eight reactions in the BBN network. We also present the temperature-dependent reaction rates based on various inputs from NLEFT and/or pionless EFT. This we consider the main systematic error of the calculation. In section 4, we present and discuss our results on the nucleon mass variations consistent with the observed abundances and the consequences for the strangeness content of the nucleon. Some technicalities are relegated to the appendices.

2 Strangeness in the nucleon

The quark mass contribution to the nucleon mass (we neglect the heavy flavors c, b here) can be derived from the mass term of the three-flavor QCD Hamiltonian,

$$\mathcal{H}_{\rm QCD}^{\rm mass} = m_u\,\bar{u}u + m_d\,\bar{d}d + m_s\,\bar{s}s\,. \tag{2.1}$$

The trace anomaly of the energy-momentum tensor $\Theta_{\mu\nu}$ allows one to quantify the effect of the quark mass terms on the nucleon mass, see e.g. refs. [20–22],

$$\langle N|\Theta_\mu^\mu|N\rangle = \left\langle N\left|-\frac{\beta(g)}{g^3}\,G^a_{\mu\nu}G^{a,\mu\nu}\right|N\right\rangle + \langle N|m_u\bar{u}u + m_d\bar{d}d + m_s\bar{s}s|N\rangle \tag{2.2}$$

where $|N\rangle$ is the nucleon spinor, β is the QCD β-function, g the strong coupling constant, $G^a_{\mu\nu}$ the non-abelian gluon field strength tensor, $a = 1,\ldots,8$ is a color index and we have neglected the anomalous dimension contribution to the quark mass term for simplicity. The first term related to the QCD gauge fields in eq. (2.2) generates the bulk of the nucleon mass, that is the nucleon mass in the three-flavor chiral limit, the famous "mass without mass" [23, 24]. The quark mass contribution to the nucleon mass is encoded in the second term in eq. (2.2), where the first two terms from the light quarks u, d are related to the well-known pion-nucleon sigma term, $\sigma_{\pi N}$, that can be precisely determined from pion-nucleon scattering data using Roy-Steiner equations. Its most recent and accurate determination including isospin-breaking effects gives $\sigma_{\pi N} = 59.0(3.5)$ MeV [25]. The strange sigma-term, that gives the strangeness contribution of the nucleon mass,

$$\sigma_s = \langle N|m_s\,\bar{s}s|N\rangle\,, \tag{2.3}$$

is known much less precisely and can be determined using lattice QCD. The FLAG group quotes an average of $\sigma_s = 44.9(6.4)$ MeV for simulations with $N_f = 2+1$ flavors and

JHEP06(2025)244

$\sigma_s = 41.0(8.8)\,\text{MeV}$ for simulations with $N_f = 2+1+1$ flavors [16]. However, looking at the individual results that enter these averages, one sees that these span a range from -40 to 160 MeV within the given uncertainties. We will therefore vary this matrix element in the range from -94 to 94 MeV, corresponding to changes of at most 10% of the nucleon mass. This variation will not only modify the nucleon mass (the proton and the neutron mass equally, since we are dealing with an isoscalar operator) but consequently also the masses of the involved nuclei. This, in turn, affects the Q-values, meaning the differences between the masses of incoming and outgoing particles, of the various reactions in the network. From imposing consistency with experimental data for primordial abundances, one can then also get bounds on the possible variations of the strange quark mass, if one assumes that the strange condensate in the nucleon remains unchanged. Note, however, that the quark masses and the condensate are scale- and scheme-dependent quantities, so that only their product is an observable. Thus, it is customary to use the $\overline{\text{MS}}$ scheme at the scale $\mu = 2\,\text{GeV}$ when one discusses the light quark masses. In what follows, we will vary the strange sigma-term and thus the nucleon mass and derive bounds on such variations from the observed primordial abundances. More precisely, if we assume the strange quark condensate to be constant, we can extract a possible variation of the strange quark mass from the nucleon mass variation via

$$|\delta_{m_s}| = \left|\frac{\Delta m_s}{m_s}\right| = \frac{\Delta m_N}{\sigma_s} \tag{2.4}$$

3 Calculational procedure

In this section, we discuss how changes in the nucleon mass affect the BBN reaction network. We heavily borrow from the formalism laid out in refs. [12, 26] and present here only the details required to investigate the influence of nucleon mass shifts on the primordial abundances.

3.1 Nucleon mass dependence of binding energies and other quantities

Fortunately, for the leading nuclear reaction $n + p \to d + \gamma$ a detailed and accurate theoretical description within the framework of pionless Effective Field Theory (EFT) exists, see refs. [27, 28]. Accordingly, one can calculate the variation of the cross section with a variation of the nucleon mass m_N and the leading effective range parameters for np-scattering: a_s, r_s, a_t, r_t denoting the singlet ($^1S_0$) scattering length, the corresponding effective range, the triplet ($^3S_1$) scattering length and corresponding effective range, respectively.

In order to determine the variation of the effective range parameters with a variation of the nucleon mass we calculated the low energy np scattering on the basis on the next-to-next-to-next-to leading order (N^{3}LO) chiral effective field theory Hamiltonian implemented on the lattice consisting of the one-pion exchange potential and various contact interactions to account for the short range behavior, similar to what was done in earlier works [29–31]. The calculation was done on a three-dimensional lattice with $L = 45$ (in lattice units) in each spatial dimension with a lattice spacing $a = 1.32\,\text{fm}$. Note that in the framework of Nuclear Lattice Effective Field Theory (NLEFT) the lattice spacing works as a regulator and is not meant to approach zero. The contact operators at given orders are listed, e.g., in [32] and the corresponding low-energy constants (LECs) were found from a fit to data for the phase shifts in the $^1S_0$ and $^3S_1 - {}^3D_1$ channels.

JHEP06(2025)244

NLEFT				
	X_0	a	b	c
a_s^{-1}	−8.3286(4) MeV	−13.437(1)	12.802(9)	−12.910(163)
r_s	2.660 53(1) fm	−0.8247(1)	0.872(1)	−0.855(15)
a_t^{-1}	36.3849(1) MeV	2.5207(1)	−2.379(2)	2.563(32)
r_t	1.740 921(1) fm	−0.652 77(1)	0.905(1)	−0.931(12)
B_d	2.208 96(9) MeV	5.276(1)	2.568(8)	−8.240(158)
Square-well potential				
a_s^{-1}	−8.310(8) MeV	−12.182(30)	11.840(212)	−8.963(3852)
r_s	2.7300(2) fm	−0.519(1)	0.498(9)	−0.377(164)
a_t^{-1}	36.4147(3) MeV	2.2105(2)	−2.141(1)	2.165(27)
r_t	1.778 992(1) fm	−0.423 76(4)	0.3949(3)	−0.403(5)
B_d	2.224 22(7) MeV	4.597(1)	1.347(6)	−5.733(117)

Table 1. Parameters for cubic polynomial fits, see eq. (3.2), to nucleon-nucleon scattering observables calculated in NLEFT or using a square-well potential. Empirical values corresponding to the parameters listed under X_0 can be found in tables 6, 8 of appendix A.

For comparison we performed the same calculation with a simple square-well potential, as earlier done e.g. in ref. [33], where the width and depth were adjusted to experimental values at the nominal nucleon mass. For details, see appendix A.

Note that in both calculations we assume the interaction to be nucleon-mass independent and the variation of the scattering parameters is due to the change of the reduced mass in the kinetic energy only. Varying the strange quark matrix element between −94 MeV to 94 MeV as described in section 2, is roughly equivalent to changing the nucleon mass by ±10%, so we define

$$m_N(\delta_{m_N}) = m_N \cdot (1 + \delta_{m_N}), \tag{3.1}$$

where $m_N = 938.92\,\text{MeV}$ is the nominal value of the average nucleon mass [34].

The variation of the effective range parameters is illustrated in figure 1. We have fitted a cubic polynomial like

$$X(\delta_{m_N}) = X_0 \cdot \left(1 + a\delta_{m_N} + b\delta_{m_N}^2 + c\delta_{m_N}^3\right) \tag{3.2}$$

to the nucleon-nucleon scattering parameters. The fit parameters and corresponding errors are listed in table 1. Note that we ignored the systematic errors in both calculations as we estimate the systematic error by the difference between the two methods.

It is worth noting that the inverse singlet scattering length changes sign for $\delta_{m_N} \simeq 9\%$ and the slope of the variation in the triplet scattering length is about half of the slope of the deuteron binding energy, consistent with the leading order result $B_d = 1/(m_N a_t^2)$. The changes in the effective range parameters are more modest, as one would also expect on dimensional grounds.

JHEP06(2025)244

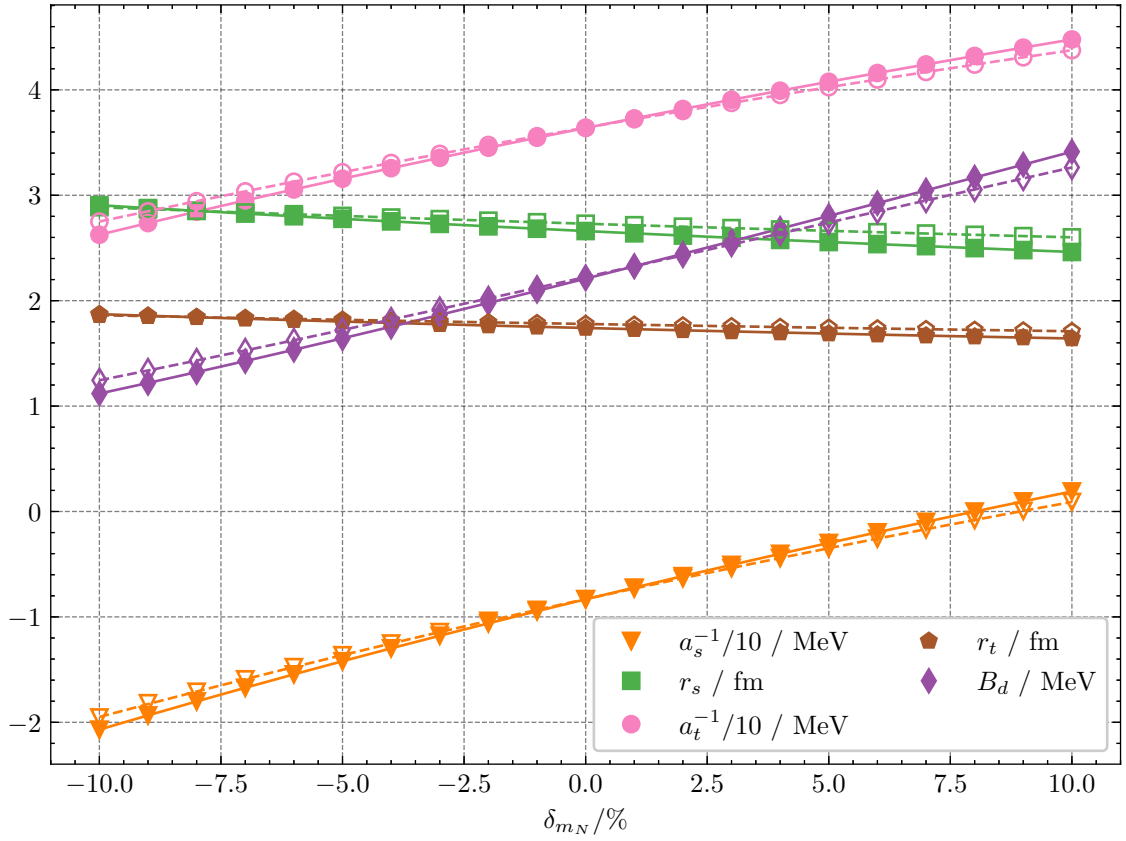

Figure 1. Variation of the np effective range expansion parameters with the nucleon mass: $m_N(\delta_{m_N}) = m_N\,(1+\delta_{m_N})$, where m_N is the nominal nucleon mass and δ_{m_N} is the fractional change; a_s is the singlet scattering length (orange), r_s is the corresponding effective range (green), a_t is the triplet scattering length (pink), r_t is the corresponding effective range (brown), B_d is the deuteron binding energy (purple). The closed symbols and solid lines refer to the NLEFT calculation of the nucleon-nucleon scattering parameters and the corresponding cubic polynomial fits, while the open symbols and dashed lines present the results obtained with the square-well potential and the corresponding fits.

The effect of changes in the nucleon mass on the $n + p \to d + \gamma$ rate as a function of the temperature is appreciable, see figure 2, in particular for temperatures well below $T_9 = 1$, with $T_9 := T/(10^9\ \mathrm{K})$. However, the $n + p \to d + \gamma$ rate is mostly relevant at high temperatures so the effect from variations in this rate on the element abundances may not be as great as suggested by the figure. The main effect from changes in the deuteron binding energy will come from the inverse rate $d + \gamma \to n + p$ as this defines the start of BBN (the deuterium bottleneck).

No detailed theoretical description is available for other nuclear reactions in the BBN network. However, we can make a statement concerning the variation of the binding energies of three- and four nucleon systems with a variation of the singlet scattering length a_s and the deuteron binding energy B_d. To this end we invoke the relations cited in eq. (5.2) in ref. [35] quoting [36]:

$$
\begin{aligned}
K^{a_s}_{B_{^3\mathrm{He}}} &= 0.12 \pm 0.01\,, & K^{B_d}_{B_{^3\mathrm{He}}} &= 1.41 \pm 0.01\,; \\
K^{a_s}_{B_{^4\mathrm{He}}} &= 0.037 \pm 0.011\,, & K^{B_d}_{B_{^4\mathrm{He}}} &= 0.74 \pm 0.22\,,
\end{aligned}
\tag{3.3}
$$

JHEP06(2025)244

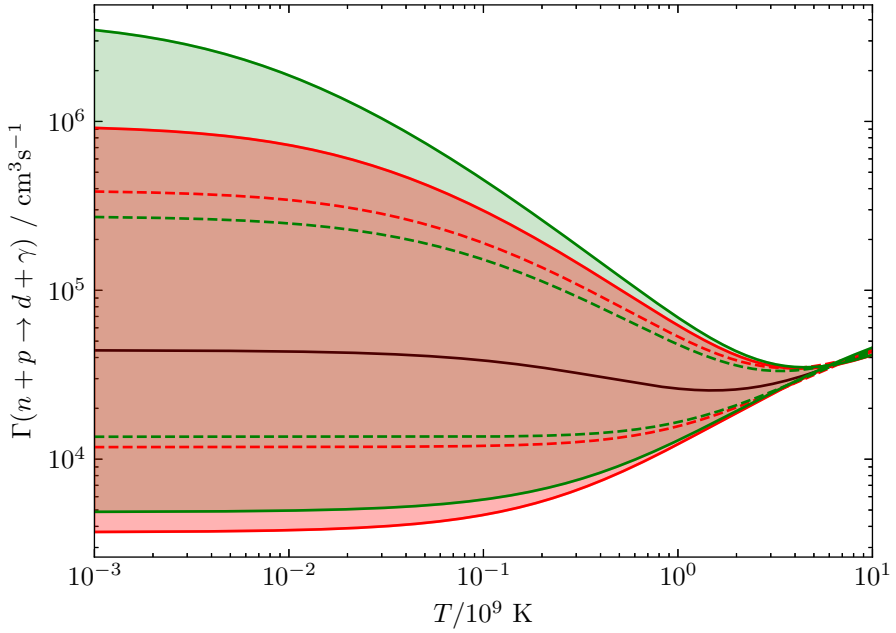

Figure 2. Variation of the rate of the $n + p \to d + \gamma$ reaction as a function of the temperature $T_9 = T/(10^9\ \mathrm{K})$. In red the variation based on the effective range parameters calculated in the NLEFT framework is shown. The green curves are the results obtained with the simple square well potential. The black curve reflects the rate calculated with the nominal mass m_N, the dashed lines correspond to $\delta_{m_N} = \pm 0.05$ and the solid lines to $\delta_{m_N} = \pm 0.10$.

where

$$K_y^x := \frac{x}{y}\frac{\Delta y}{\Delta x}\,. \tag{3.4}$$

From the parameter fits listed in table 1 and displayed in figure 1 we find for the NLEFT calculation

$$K_{a_s}^{m_N} = -K_{1/a_s}^{m_N} = 13.437 \pm 0.001\,, \qquad K_{B_d}^{m_N} = 5.276 \pm 0.001\,, \tag{3.5}$$

and from the results obtained with the square-well potential

$$K_{a_s}^{m_N} = -K_{1/a_s}^{m_N} = 12.18 \pm 0.03\,, \qquad K_{B_d}^{m_N} = 4.597 \pm 0.001\,. \tag{3.6}$$

We then obtain

$$\begin{aligned} K_{B_{^3\mathrm{He}}}^{m_N} &= K_{a_s}^{m_N} K_{B_{^3\mathrm{He}}}^{a_s} + K_{B_d}^{m_N} K_{B_{^3\mathrm{He}}}^{B_d} = 9.05 \pm 0.14\,, \\ K_{B_{^4\mathrm{He}}}^{m_N} &= K_{a_s}^{m_N} K_{B_{^4\mathrm{He}}}^{a_s} + K_{B_d}^{m_N} K_{B_{^4\mathrm{He}}}^{B_d} = 4.4 \pm 1.2\,, \end{aligned} \tag{3.7}$$

from the NLEFT np-parameters and for the square-well potential calculation

$$\begin{aligned} K_{B_{^3\mathrm{He}}}^{m_N} &= K_{a_s}^{m_N} K_{B_{^3\mathrm{He}}}^{a_s} + K_{B_d}^{m_N} K_{B_{^3\mathrm{He}}}^{B_d} = 7.94 \pm 0.13\,, \\ K_{B_{^4\mathrm{He}}}^{m_N} &= K_{a_s}^{m_N} K_{B_{^4\mathrm{He}}}^{a_s} + K_{B_d}^{m_N} K_{B_{^4\mathrm{He}}}^{B_d} = 3.9 \pm 1.0\,. \end{aligned} \tag{3.8}$$

Although the resulting K-factors for ^{3}He differ by about 10%, in the case of ^{4}He, the K-factors agree within the uncertainties. We note that these are approximate relations,

JHEP06(2025)244

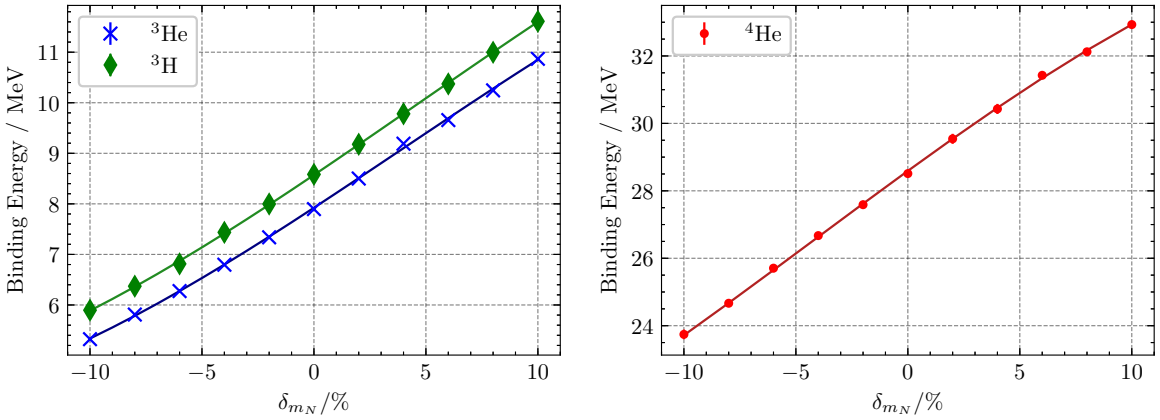

Figure 3. The binding energies for the three-nucleon system (left) and Helium-4 (right) calculated in the framework of NLEFT for a variation of the nucleon mass, δ_{m_N}, between ±10%. The solid lines are the corresponding cubic polynomial fits to the data, as given in eq. (3.2).

as they ignore any effective range effects in the binding energies of the light nuclei. Using these K-factors, we find for the change of the binding energy as a function of the change in the nucleon mass in linear approximation

$$\Delta B_{^3\mathrm{He}} = \frac{B_{^3\mathrm{He}}}{m_N} K^{m_N}_{B_{^3\mathrm{He}}} \Delta m_N$$

and thus

$$B_{^3\mathrm{He}}(\delta_{m_N}) = B_{^3\mathrm{He}} \left(1 + K^{m_N}_{B_{^3\mathrm{He}}} \delta_{m_N}\right) ,$$

where $\delta_{m_N} := \Delta m_N / m_N$ is the fractional change in the nucleon mass. Likewise

$$B_{^4\mathrm{He}}(\delta_{m_N}) = B_{^4\mathrm{He}} \left(1 + K^{m_N}_{B_{^4\mathrm{He}}} \delta_{m_N}\right) .$$

In both cases the dependence via the deuteron binding energy dominates.

Alternatively, we calculated the variation of the binding energies of the three and four nucleon system within NLEFT. In both cases the same action as described in [37] is used, and the binding energies are calculated on a lattice with $L = 10$ (in lattice units) in each spatial dimension and a lattice spacing $a = 1.32\,\mathrm{fm}$. For the three nucleon system, we calculate the binding energies non-perturbatively, while for the binding energy of Helium-4 we do various simulations for different values of the Euclidean time (for more details on Euclidean time projection, see, e.g., [38]) so that we can extrapolate to infinite times. As for the calculation of the deuteron binding energy variation, we only varied the nucleon mass in the kinetic energy, the interactions in the Hamiltonian were not changed. The results are displayed in figure 3.

Similar to the nucleon-nucleon scattering observables, we have fitted a cubic polynomial (see eq. (3.2)) to the binding energy data obtained in the NLEFT framework. The corresponding fit parameters are listed in table 2. The parameter of the term linear in δ_{m_N} is then the K-value defined in eq. (3.4)) as introduced e.g. in [36]. A comparison of the results obtained within this framework:

$$K^{m_N}_{B_{^3\mathrm{H}}} = 3.477(39), \quad K^{m_N}_{B_{^3\mathrm{He}}} = 3.662(66), \quad K^{m_N}_{B_{^4\mathrm{He}}} = 1.685(25), \tag{3.9}$$

JHEP06(2025)244

	X_0 / MeV	a	b	c
^{3}H	8.571(12)	3.477(39)	2.011(272)	−14.490(5034)
^{3}He	7.923(19)	3.662(66)	2.152(458)	−18.313(8460)
^{4}He	28.591(28)	1.685(25)	−0.930(170)	−7.367(3453)

Table 2. Parameters for cubic polynomial fits (see eq. (3.2)) to the three-nucleon system and Helium-4 binding energies calculated in the framework of NLEFT.

with the K-factors quoted in eqs. (3.7)–(3.8) shows that the dependence on δ_{m_N} is significantly smaller than what was found on the basis of the results from [35] and [36], especially for the three-nucleon system. We have ignored the systematic uncertainties in the NLEFT calculations (truncation error of perturbative expansion, lattice spacing dependence etc.), because as we can see, the systematic uncertainty from modeling the nucleon mass dependence as discussed here is considered to be more significant. We stress again that while the K-factors from the NLEFT calculation are exact (modulo higher order corrections), the ones based on pionless EFT are subject to effective range corrections and thus turn out to be larger in size.

These results are then used to calculate the variation of the Q-values for some relevant reactions involving these nuclei. The Q-values in turn affect the kinematics of the reactions, the reaction rate, the rates of the inverse reactions as well as Coulomb penetration factors as will be explained below.

3.2 Modeling the nucleon mass dependence of nuclear reaction rates

Based on the variation of the masses m_i (or, equivalently, of the binding energies B_i) of the nuclei ^{2}H, ^{3}H, ^{3}He and ^{4}He with the nucleon mass, we modeled the variation of the rates of reactions involving these nuclei similar to the procedure we outlined in a previous paper on the variation with the electromagnetic fine structure constant, see ref. [12] for more details:

First of all a variation of masses in a reaction of the form $a + b \to c + d$ trivially leads to a variation of the reduced masses $\mu_{ab} = m_a\, m_b/(m_a + m_b)$ and $\mu_{cb} = m_c\, m_d/(m_c + m_d)$ in the entrance and exit channels. In addition, the Q-value of the reaction

$$Q := m_a + m_b - m_c - m_d = B_c + B_d - B_a - B_b \tag{3.10}$$

is affected. These two quantities enter the nuclear reactions rates as follows:

- The temperature dependent reaction rate that follows from the energy dependent total cross section via

$$\Gamma_{ab\to cd}(T) = N_A \sqrt{\frac{8}{\pi\, \mu_{ab} (k_B T)^3}} \int_0^\infty \mathrm{d}E\, E\, \sigma_{ab\to cd}(E)\, \exp\left[-\frac{E}{k_B T}\right] \tag{3.11}$$

  depends on μ_{ab}. Here E is the center-of mass kinetic energy, N_A denotes Avogadro's number and k_B is Boltzmann's constant;

- The reaction rate for the inverse reaction then depends on the reduced masses and the Q-value as

$$\Gamma_{cd\to ab}(T) = \left(\frac{\mu_{ab}}{\mu_{cd}}\right)^{\frac{3}{2}} \frac{g_a\, g_b}{g_c\, g_d}\, \exp\left[-\frac{Q}{k_B T}\right] \Gamma_{ab\to cd}(T)\,, \tag{3.12}$$

  where g_i denotes the spin multiplicity of particle i;

JHEP06(2025)244

- We shall assume that the cross section for a strong reaction $a + b \to c + d$ depends on m_N as

$$\sigma_{ab\to cd}(E; m_N) = \sqrt{E + Q(m_N)}\, P_i(x_i(E, m_N))\, P_f(x_f(E, m_N))\, f(E) \tag{3.13}$$

where f is some function independent of m_N and $P_i(x_i)$, $P_f(x_f)$ are penetration factors of the form

$$P(x) = \frac{x}{\exp\{x\} - 1}\,, \tag{3.14}$$

reflecting the Coulomb repulsion in a channel where both particles are charged. The first factor in equation (3.13) accounts for the exit channel momentum dependence of the cross section of the strong reaction $a + b \to c + d$. Here,

$$x_i(E, m_N) = \sqrt{\frac{E_G^i(m_N)}{E}}\,, \qquad x_f(E, m_N) = \sqrt{\frac{E_G^f(m_N)}{E + Q(E)}}\,, \tag{3.15}$$

with, denoting the charge number of nuclide k by Z_k and the fine structure constant by α,

$$E_G^i = 2\,\pi^2\, Z_a^2\, Z_b^2\, \mu_{ab}\, \alpha^2\,, \quad E_G^f = 2\,\pi^2\, Z_c^2\, Z_d^2\, \mu_{cd}\, \alpha^2 \tag{3.16}$$

the Gamow-energies in the entrance and the exit channel, respectively. Thus the cross section is supposed to depend on the varying nucleon mass $m_N(\delta_{m_N}) = m_N\,(1 + \delta_{m_N})$, where m_N is the nominal nucleon mass and δ_{m_N} the fractional change, as

$$\begin{aligned}\sigma_{ab\to cd}(E; m_N(\delta_{m_N})) = {} & \frac{P_i(x_i(E, m_N(\delta_{m_N})))}{P_i(x_i(E, m_N))}\, \frac{\sqrt{E + Q(m_N(\delta_{m_N}))}}{\sqrt{E + Q(m_N)}}\, \frac{P_f(x_f(E, m_N(\delta_{m_N})))}{P_f(x_f(E, m_N))} \\ & \times \quad \sigma_{ab\to cd}(E; m_N)\,.\end{aligned} \tag{3.17}$$

For a radiative capture reaction $a + b \to c + \gamma$ the corresponding expression is

$$\sigma_{ab\to c\gamma}(E; m_N(\delta_{m_N})) = \frac{P_i(x_i(E, m_N(\delta_{m_N})))}{P_i(x_i(E, m_N))} \left(\frac{E + Q(m_N(\delta_{m_N}))}{E + Q(m_N)}\right)^3 \sigma_{ab\to c\gamma}(E; m_N)\,, \tag{3.18}$$

where the second factor reflects the final state momentum dependence assuming dipole dominance of the radiation.

Considering exclusively the variations for the reactions including only d, ^{3}H, ^{3}He and ^{4}He is justified as these are the reactions most relevant for the abundances of these light nuclei, as was shown, e.g., in [39]. In order to derive constraints on the nucleon mass variation, we will use experimental data collected on the abundances by the Particle Data Group (PDG) [34] for deuterium and Helium-4, because these are the most reliable (for Lithium-7 the so-called "Lithium problem" exists [40], which makes it unsuitable for these kinds of considerations). The binding energy dependence on the nucleon mass for other light nuclei is not known, so it would seem incomplete (and unnecessary) to change the Q-values of other reactions that include the four lightest but also other nuclei. Including the first reaction $n + p \to d + \gamma$ which was already discussed in section 3.1, there are eight reactions where

JHEP06(2025)244

only the four lightest nuclei are involved. In figure 4, the variation of these rates resulting from changing the nucleon mass by $\pm 10\%$ is displayed for the temperature range in which these reactions are most relevant in the BBN process as explained in [41]. Here, we have used an updated version (compared to [12]) of the parameterizations of cross sections for 17 key rates which are listed in appendix B.

We have defined "flags" corresponding to different combinations of how we calculated the nucleon-nucleon scattering parameters and the changes in the binding energies:

- $(0, 0)$ means everything is based on NLEFT calculations (see the upper part of table 1 and table 2);
- $(0, 1)$ is the NLEFT result for the nucleon-nucleon parameters (see the upper part of table 1) combined with variations of the binding energies from pionless EFT [36] (see eq. (3.7));
- $(1, 0)$ uses the square-well results for the np scattering parameters (see the lower part of table 1) combined with the three- and four-body binding energies from NLEFT (table 2);
- $(1, 1)$ is again the np scattering parameters (see the lower part of table 1) from the square-well potential now combined with the K-factors from pionless EFT [36] (see eq. (3.8)).

For some of these combinations, the Q-values for some reactions become negative for certain δ_{m_N} meaning the reactions is not kinematically allowed anymore. In this case, we have simply set the reaction rate to zero.

4 Results and discussion

The variation of the resulting relative abundances for the nuclides ^{2}H, ^{3}H + ^{3}He, ^{4}He, ^{6}Li and ^{7}Li + ^{7}Be with a variation of the nucleon mass, cf. eq. (3.1) is displayed in figure 6. These results were obtained by varying the rates of the eight reactions discussed above with modified (see [12, 26]) versions of

- the Kawano code [42] `nuc123`,
- `PRyMordial` [10],
- `AlterBBN` [43, 44] and
- `PRIMAT` [41].

The nominal abundances, i.e. without variation of the nucleon mass are compared to experimental data in table 3. As mentioned in the last section, some reaction Q-values become negative for too large negative variations of the nucleon mass for some of the model versions we used for varying the nucleon-nucleon scattering parameters and binding energies. For the reaction $d(d, n)^3$He this happens below $\delta_{m_N} = -7\%$ (flag $(0, 1)$), other reactions become kinematically forbidden at larger (negative) changes in the nucleon mass. Because the system

JHEP06(2025)244

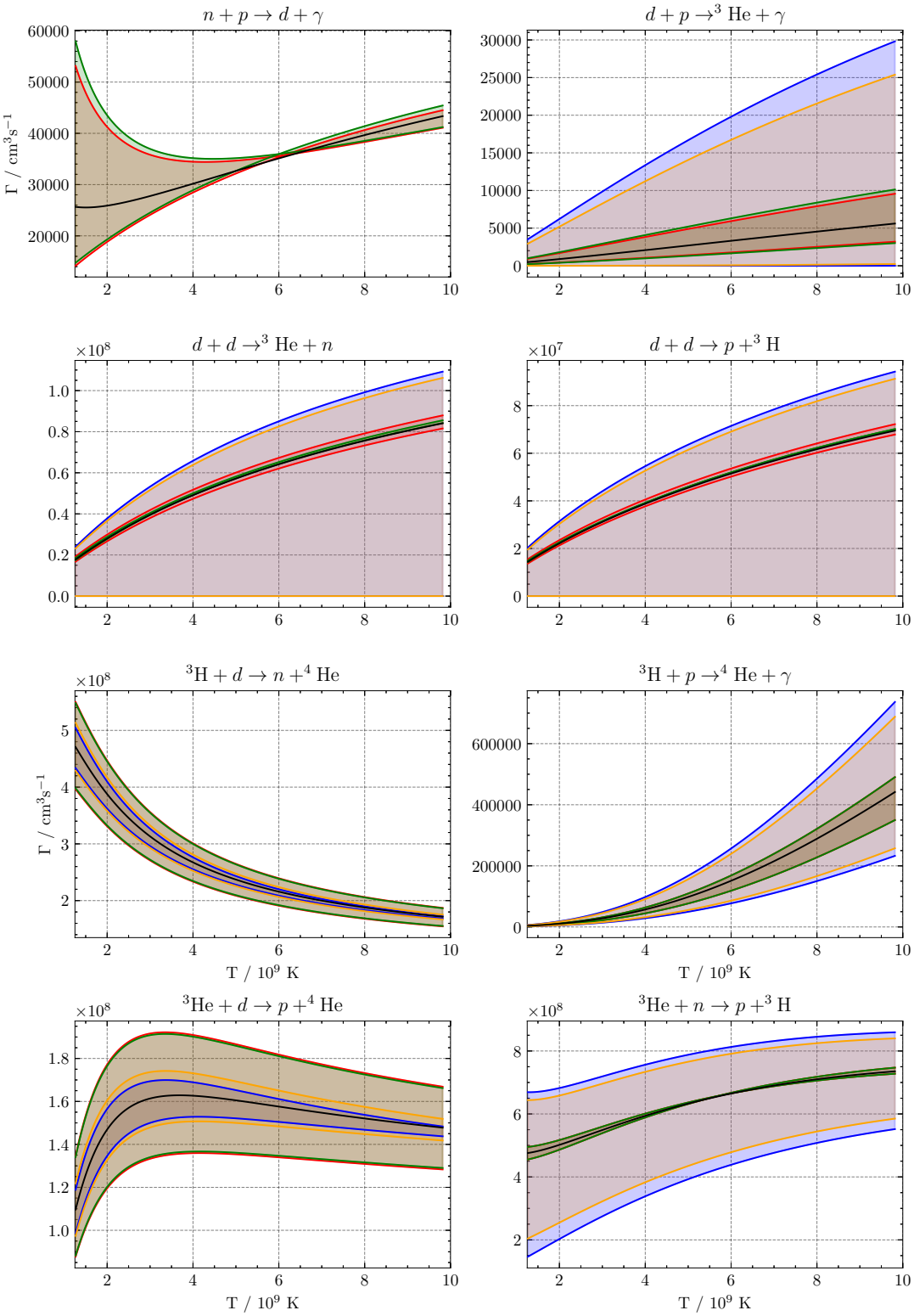

Figure 4. Reaction rates of the eight reactions in the BBN network involving only d, ^{3}H, ^{3}He and ^{4}He. The nominal value of the rates according to [28] (for $n + p \to d + \gamma$) or to the parameterizations listed in appendix B is given in black. The bands correspond to a nucleon mass variation of $\pm 10\%$. Red: $(0, 0)$; blue: $(0, 1)$; green: $(1, 0)$; orange: $(1, 1)$, where the combinations 0 and 1 refer to the flags defined at the end of section 3.

JHEP06(2025)244

	Y_d/Y_H	$Y_{^3\mathrm{H}+^3\mathrm{He}}/Y_H$	Y_P	$Y_{^6\mathrm{Li}}/Y_H$	$Y_{^7\mathrm{Li}+^7\mathrm{Be}}/Y_H$
`nuc123`	2.452×10^{-5}	1.078×10^{-5}	0.246	0.960×10^{-14}	5.035×10^{-10}
`PRyMordial`	2.541×10^{-5}	1.092×10^{-5}	0.247	0.920×10^{-14}	4.874×10^{-10}
`AlterBBN`	2.563×10^{-5}	1.096×10^{-5}	0.247	1.027×10^{-14}	4.756×10^{-10}
`PRIMAT`	2.517×10^{-5}	1.089×10^{-5}	0.247	0.994×10^{-14}	4.874×10^{-10}
PDG [34]	$2.547(29) \times 10^{-5}$		0.245(3)		$1.6(3) \times 10^{-10}$

Table 3. Values of the light element abundances as calculated with the four codes for the nominal value of the nucleon mass m_N and the corresponding experimental value from [34]. For ^{4}He the mass fraction is given.

		`nuc123`		`PRyMordial`		`AlterBBN`		`PRIMAT`	
Flag		$\delta_{m_N,\mathrm{min}}$	$\delta_{m_N,\mathrm{max}}$	$\delta_{m_N,\mathrm{min}}$	$\delta_{m_N,\mathrm{max}}$	$\delta_{m_N,\mathrm{min}}$	$\delta_{m_N,\mathrm{max}}$	$\delta_{m_N,\mathrm{min}}$	$\delta_{m_N,\mathrm{max}}$
0	0	-0.00204	-0.00105	-0.00060	0.00039	-0.00023	0.00075	-0.00099	-0.00002
0	1	-0.00127	-0.00065	-0.00037	0.00024	-0.00014	0.00047	-0.00062	-0.00001
1	0	-0.00235	-0.00126	-0.00066	0.00043	-0.00025	0.00082	-0.00109	-0.00002
1	1	-0.00154	-0.00082	-0.00043	0.00028	-0.00017	0.00054	-0.00072	-0.00001

Table 4. Constraints on the nucleon mass variation δ_{m_N} from comparing the simulated deuterium abundance for different values of m_N to the experimental value $2.547(29) \times 10^{-5}$ [34], for the different methods of deriving the nucleon-nucleon scattering parameters and binding energies and for the different codes used to simulate BBN.

of differential equations becomes somewhat numerically unstable, the codes do not give reliable results in these cases, so we only included values for $\delta_{m_N} \geq -7\%$ for the flags $(0,1)$ and $(1,1)$ in figure 6. We did not study this in more detail or tried to include possible effects of other reaction channels opening up for large negative changes in the nucleon mass because the deuteron abundance alone constraints the region of interest for variations in m_N to the sub-percent-level, where these kinds of considerations are not relevant. Of course, whenever a Q-value becomes negative, the reaction would effectively proceed in the reverse direction, which could significantly affect certain abundances. In our case, notable differences would be expected particularly in the abundances of elements with $A = 3$, since the first reactions to develop negative Q-values for negative δ_{m_N} are the d-d reactions that produce tritium and He-3. Indeed, the overall structure of BBN would change substantially. While it would be fascinating to explore the impact of such effects on the BBN network, this topic warrants a dedicated study and would be best presented in a separate publication, as we cannot do it justice here.

On the basis of the uncertainties of the empirical data for the relative deuteron abundance, $Y_{^2\mathrm{H}} = (2.547 \pm 0.029) \times 10^{-5}$ [34], and the relative ^{4}He (mass) abundance, $Y_{^4\mathrm{He}} = 0.245 \pm 0.003$ [34], we estimated the possible variation of the nucleon mass with the four combinations of the rates discussed in section 3. The resulting ranges in the relative nucleon mass variation δ_{m_N} are displayed in figure 5 and listed in table 4 for ^{2}H and in table 5 for ^{4}He.

JHEP06(2025)244

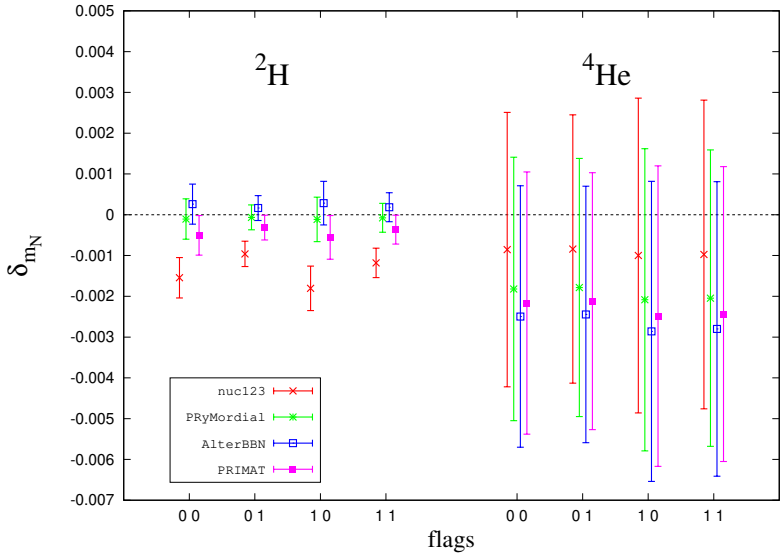

Figure 5. Extracted ranges of δ_{m_N} for the four rate combinations labeled "0 0", "0 1", "1 0" and "1 1" discussed in section 3, both on the basis of the ^{2}H (left) and the ^{4}He (right) abundance data. The results with the BBN code `nuc123` is displayed by red crosses, with `PRyMordial` by green stars, with `AlterBBN` with blue open squares and with `PRIMAT` by magenta filled squares.

		nuc123		PRyMordial		AlterBBN		PRIMAT	
Flag		$\delta_{m_N,\min}$	$\delta_{m_N,\max}$	$\delta_{m_N,\min}$	$\delta_{m_N,\max}$	$\delta_{m_N,\min}$	$\delta_{m_N,\max}$	$\delta_{m_N,\min}$	$\delta_{m_N,\max}$
0	0	-0.00422	0.00251	-0.00505	0.00141	-0.00570	0.00071	-0.00538	0.00105
0	1	-0.00413	0.00245	-0.00495	0.00138	-0.00559	0.00070	-0.00527	0.00103
1	0	-0.00486	0.00286	-0.00579	0.00162	-0.00654	0.00082	-0.00617	0.00120
1	1	-0.00476	0.00281	-0.00568	0.00159	-0.00641	0.00081	-0.00605	0.00118

Table 5. Constraints on the nucleon mass variation δ_{m_N} from comparing the simulated Helium-4 mass fraction for different values of m_N to the experimental value 0.245(3) [34], for the different methods of deriving the nucleon-nucleon scattering parameters and binding energies and for the different codes used to simulate BBN.

From this we infer that $\delta_{m_N} \in (-0.0024, +0.0008)$ and $\delta_{m_N} \in (-0.0065, +0.0029)$, on the basis of $Y_{^2\mathrm{H}}$ and $Y_{^4\mathrm{He}}$, respectively. This is all well below 1%. It is amusing to observe, see the bottom panel in figure 6, that a decrease in the nucleon mass by $1-2\%$ apparently would solve the so called "Lithium-problem", but such a variation is of course excluded by the other relative abundance data mentioned before. The main contribution to the ^{7}Be abundance comes from the reaction $^4\mathrm{He} + {}^3\mathrm{He} \to {}^7\mathrm{Be} + \gamma$ (see figure B7 of [39]). The ^{4}He abundance decreasing sizeably for negative δ_{m_N} is the reason why also the ^{7}Be abundance decreases to the experimentally observed value and then even further. For the abundances of ^{6}Li and $^3\mathrm{He} + {}^3\mathrm{H}$ a strong non-linear dependence on the nucleon mass is found, while also the four versions of the rates yield markedly varying results for the abundances, but unfortunately there are no reliable empirical data for these nuclides.

JHEP06(2025)244

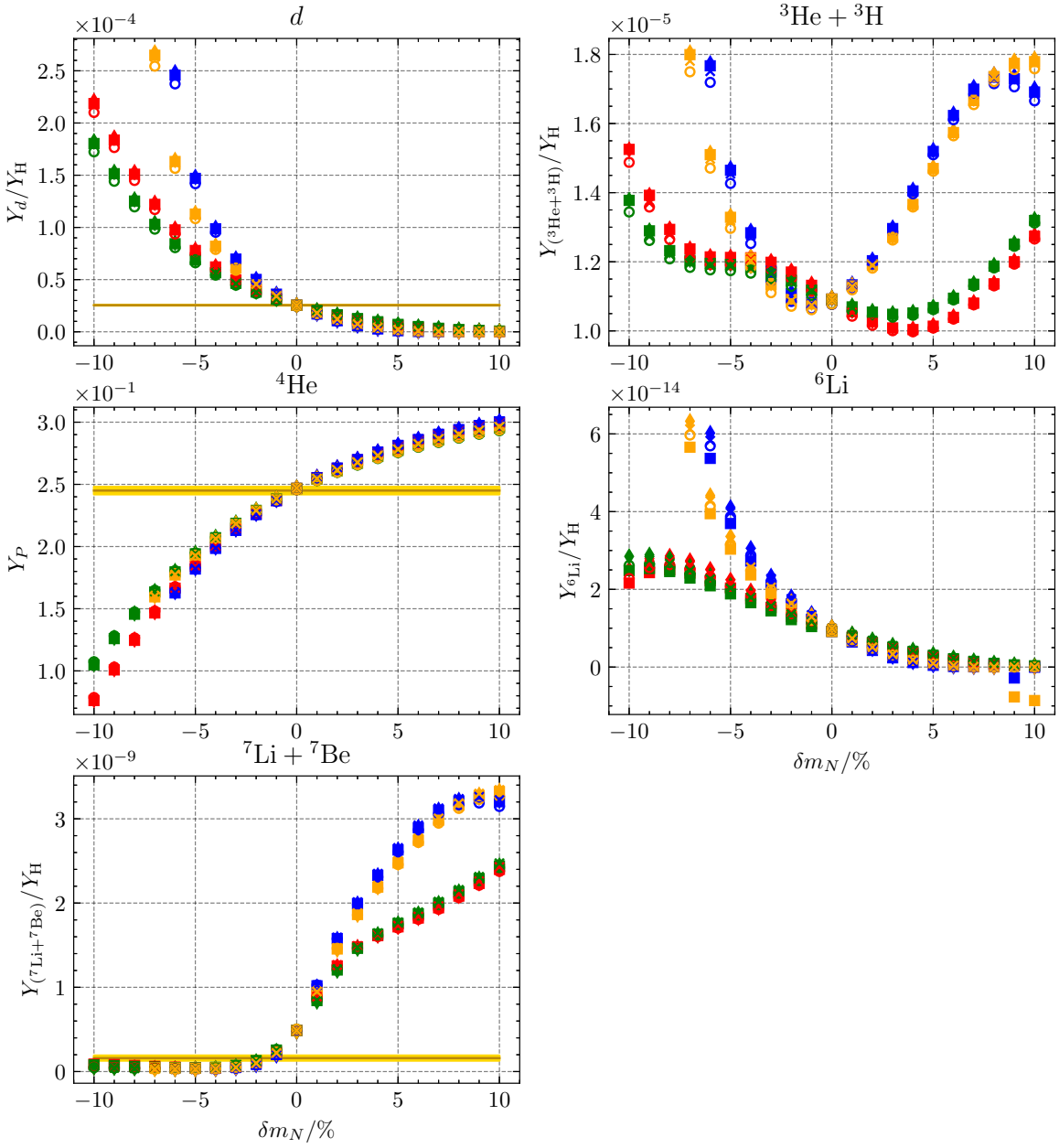

Figure 6. Nucleon mass dependence of the relative abundances for ^{2}H, ^{3}H+He, ^{4}He, ^{6}Li and ^{7}Li+Be calculated with a modified verion of the Kawano code `nuc123` [42] (open circles), with `PRyMordial` [10] (squares), with `AlterBBN` [43, 44] (diamonds) and with `PRIMAT` [41] (crosses). For ^{4}He this is the mass ratio with respect to hydrogen, for the other nuclides the relative abundance reflects the number ratio with respect to hydrogen. The color coding of the curves, respective to the different methods, is the same as in figure 4.

JHEP06(2025)244

We can now draw conclusions on the size of the variation of the strangeness content and the strange quark mass. Taking the largest possible variation (in size) from tables 4, 5, we see that $|\Delta m_N|$ is bounded by 2.3 MeV and 6.1 MeV from the deuterium and the ^{4}He abundance, respectively. This translates into possible variations of σ_s of less than 5.1% and 13.6%, respectively, using the central FLAG value for $N_f = 2 + 1$ flavors. As in the case of variations of the Higgs VEV [14], the deuterium abundance sets the stronger bound. Assuming that the strange quark condensate does not change, we can derive an upper bound on variation of the strange quark mass (from the deuterium abundance)

$$\left|\frac{\Delta m_s}{m_s}\right| \leq 5.1\% \,. \tag{4.1}$$

Note, however, that this is only an upper bound. Scanning through tables 4, 5, one can see that the range of possible variations for the individual codes is much smaller. The interval of possible values for δ_{m_N} that we mention is only as large because the nominal value of the abundances vary between the codes (see also figure 5). In addition, if we would take the largest values of δ_{m_N} found from NLEFT calculations only (flag $(0,0)$), which, in our opinion, is the best calculation, the upper bound for the variation of the strange quark mass would reduce further by 1%. Furthermore, assuming that the Yukawa couplings do not vary, one can also derive a bound on possible variations of $\Lambda_{\rm QCD}$. For that, we use eq. (A.2) from ref. [13] together with the bound in eq. (4.1), it follows that $\Lambda_{\rm QCD}$ varied by less than 1.13% between the time of the Big Bang and now.

Acknowledgments

We thank Serdar Elhatisari and Fabian Hildenbrand for help with the NLEFT simulations. The authors gratefully acknowledge the computing time granted by the John von Neumann Institute for Computing (NIC) and provided on the supercomputer JURECA [45] at Jülich Supercomputing Centre (JSC). This work was supported in part by the European Research Council (ERC) under the European Union's Horizon 2020 research and innovation programme through the ERC AdG EXOTIC (grant agreement No. 101018170). The work of UGM was supported in part by the CAS President's International Fellowship Initiative (PIFI) (Grant No. 2025PD0022).

A Square-well potentials

The stationary radial Schrödinger equation for non-relativistic S-wave relative motion of two nucleons of mass m_N in a spherical potential well of depth $-V_0$ and width R_0:

$$V(r) = \begin{cases} -V_0 \,, \; r < R_0 \,, \\ \quad 0 \,, \; r > R_0 \end{cases} \,, \tag{A.1}$$

reads

$$-\frac{1}{2\mu}\, u''(r) + V(r)\, u(r) = E\, u(r) \tag{A.2}$$

where $\mu = m_N/2$ is the reduced mass and E the energy. Defining the dimensionless potential strength

$$\xi^2 := 2\,\mu\, V_0\, R_0^2 \,, \tag{A.3}$$

JHEP06(2025)244

proton mass	m_p [MeV]	938.27208816
neutron mass	m_n [MeV]	939.56542052
reduced mass	μ [MeV]	469.45915448
nucleon mass	m_N [MeV]	938.91875434
depth	V_0 [MeV]	33.306
radius	R_0 [fm]	2.116

Table 6. Spherical well parameters for the ${}^3S_1$ channel.

		calc.	exp. [46].
inverse scattering length	a_t^{-1} [MeV]	36.414	36.407(7)
effective range	r_t [fm]	1.779	1.753(2)
binding energy	B [MeV]	2.224433	2.224575(9)
asymptotic normalisation	A_s [fm$^{-\frac{1}{2}}$]	0.879	0.8845(8)
root mean square radius	r_d [fm]	1.9505	1.9676(10)

Table 7. Deuteron properties and low-energy scattering parameters for the ${}^3S_1$ channel.

the scattering length a and the effective range r are given by the expressions:

$$a = R_0\,\alpha(\xi) := R_0\left(1 - \frac{\tan\xi}{\xi}\right), \qquad r = R_0\left(1 - \frac{1}{\alpha(\xi)\,\xi^2} - \frac{1}{3\,\alpha(\xi)^2}\right). \tag{A.4}$$

Accordingly, for given a and r the value of $\xi^2 \propto V_0\,R_0^2$ follows from the ratio r/a and R_0 from the first equation in (A.4). For a bound state $\xi > 1$ and with x the solution of $\sin(x)/x = 1/\xi$ the binding energy B is given by

$$B = \frac{1}{2\,\mu\,R_0^2}\left(\xi^2 - x^2\right).$$

Application to the np-${}^3S_1$ channel. In this simple model we consider S-wave scattering only and thus neglect the ${}^3S_1 - {}^3D_1$ mixing. The low energy triplet scattering parameters (scattering length a_t and effective range r_t) can e.g. be found in ref. [46]. With the spherical well parameters listed in table 6. we find with the values for the scattering length and effective range as listed in the column labeled "calc." in table 7, a fair description of various empirical deuteron data, also listed in table 7.

Application to the np-${}^1S_0$ channel. We have inspected three parameter sets, based on three combinations of (a_s, r_s) (the ${}^1S_0$ scattering length and effective range, respectively), as listed in table 8, that, via eq. (A.4) lead to the potential parameters V_0 and R_0 listed in the last two columns of this table. Keeping the potential parameters fixed to the values of tables 6, 8 (second line labeled "Pionless EFT") by varying the nucleon mass as $m_N(\delta_{m_N}) = m_N\,(1+\delta_{m_N})$ the variation of the scattering parameters and the deuteron binding energy is as shown in figure 1.

JHEP06(2025)244

	a_s^{-1} [MeV]	r_s [fm]	V_0 [MeV]	R_0 [fm]
Experiment [47]	-8.312(7)	2.77(5)	13.358	2.650
Pionless EFT [28]	-8.309	2.73	13.752	2.614
CD-Bonn [47]	-8.313	2.671	14.376	2.558

Table 8. Scattering parameters and spherical well parameters for the $^1S_0$ channel.

B Parameterizations of cross sections

In this appendix we present updated parameterizations for 17 relevant cross sections in BBN. Compared to the parameterizations shown in [12], we have slightly changed a few parameters and added error estimations. Because of its more modest variation with the centre-of-mass (CMS) energy E, one often prefers to parameterize the so-called S-factor

$$S(E) = \sigma(E) \cdot E \cdot e^{\sqrt{E_G/E}} \tag{B.1}$$

over the cross section $\sigma(E)$. Here the Gamow-energy E_G is

$$E_G = 2\pi^2 \mu_{ab} c^2 Z_a^2 Z_b^2 \alpha^2, \tag{B.2}$$

and the S-factor was chosen to be a rational function in terms of the CMS energy E (given here in MeV) multiplied by a constant S_0 (in MeV mb):

$$S(E) = S_0 \frac{1 + a_1 E + a_2 E^2 + a_3 E^3}{1 + q_1 E + q_2 E^2 + q_3 E^3}. \tag{B.3}$$

The constant S_0 and the coefficients a_k, q_k in $(\text{MeV})^{-k}$ are given in tables 9 and 10 for 14 charged particle reactions.
For neutron capture reactions we parameterize a function

$$\mathcal{R}(E) = \sigma(E)\sqrt{E} \tag{B.4}$$

similarly to the S-factor above as

$$\mathcal{R}(E) = \mathcal{R}_0 \frac{1 + a_1 E + a_2 E^2 + a_3 E^3}{1 + q_1 E + q_2 E^2 + q_3 E^3}, \tag{B.5}$$

with E in MeV, the coefficients a_k, q_k in $(\text{MeV})^{-k}$ and $\mathcal{R}_0$ in $(\text{MeV})^{1/2}$mb. The S-factor is then for neutron-capture reactions

$$S(E) = \mathcal{R}(E) \cdot \sqrt{E} = \sigma(E) \cdot E. \tag{B.6}$$

There are some reactions with resonances in the energy range considered here. For these, we can parameterize the S-factor as a rational function or a polynomial with a combination of (relativistic) Breit-Wigner functions. The coefficients for the relativistic Breit-Wigner functions (E, Γ, M in MeV) of the form

$$\text{BW}(E; k, \Gamma, M) = \frac{k}{\Gamma^2 M^2 + (E^2 - M^2)^2} \tag{B.7}$$

JHEP06(2025)244

Reaction	S_0	a_1	a_2	a_3	q_1	q_2	q_3
$d + p \to {}^3\mathrm{He} + \gamma$	$(2.072 \pm 0.043) \times 10^{-4}$	30.094 ± 1.839	16.754 ± 2.302	0	0	0.035 ± 0.008	0
$d + {}^4\mathrm{He} \to {}^6\mathrm{Li} + \gamma$	$(4.382 \pm 1.762) \times 10^{-7}$	0	90.682 ± 37.560	0	0	0	0
${}^3\mathrm{H} + p \to {}^4\mathrm{He} + \gamma$	$(1.875 \pm 0.031) \times 10^{-3}$	10.773 ± 0.996	32.613 ± 7.711	113.840 ± 4.597	0	0	$8.919 \pm 0.181 \times 10^{-3}$
${}^3\mathrm{H} + {}^4\mathrm{He} \to {}^7\mathrm{Li} + \gamma$	$(9.275 \pm 0.258) \times 10^{-2}$	-0.937 ± 0.067	0.594 ± 0.064	0	0	0	0
${}^3\mathrm{He} + {}^4\mathrm{He} \to {}^7\mathrm{Be} + \gamma$	$(5.160 \pm 0.161) \times 10^{-1}$	-0.556 ± 0.064	0.281 ± 0.060	0	0	0.132 ± 0.051	0
${}^6\mathrm{Li} + p \to {}^7\mathrm{Be} + \gamma$	$(3.208 \pm 0.619) \times 10^{-2}$	40.354 ± 9.384	-11.448 ± 1.107	0	-9.092 ± 0.616	24.154 ± 3.089	0

Table 9. Fit parameters according to eq. (B.3) and eq. (B.9) for some relevant radiative capture reactions. S_0 is given in MeV mb, a_k, q_k in $(\mathrm{MeV})^{-k}$.

Reaction	S_0	a_1	a_2	a_3	q_1	q_2
$d + d \to {}^3\mathrm{He} + n$	$(5.517 \pm 0.131) \times 10^1$	6.701 ± 0.377	0	0	0.531 ± 0.044	-0.032 ± 0.005
$d + d \to p + {}^3\mathrm{H}$	$(5.786 \pm 0.088) \times 10^1$	3.443 ± 0.321	0	0	0.149 ± 0.034	0
${}^3\mathrm{H} + d \to n + {}^4\mathrm{He}$	$(1.069 \pm 0.031) \times 10^4$	-0.994 ± 1.342	11.819 ± 5.744	0	-24.260 ± 0.444	243.991 ± 8.442
${}^3\mathrm{He} + d \to p + {}^4\mathrm{He}$	$(5.937 \pm 0.052) \times 10^3$	-2.049 ± 0.175	3.835 ± 0.296	-0.305 ± 0.063	-6.788 ± 0.053	15.604 ± 0.223
${}^6\mathrm{Li} + p \to {}^3\mathrm{He} + {}^4\mathrm{He}$	$(2.162 \pm 0.076) \times 10^3$	-0.058 ± 0.008	0	0	0	0
${}^7\mathrm{Li} + p \to {}^4\mathrm{He} + {}^4\mathrm{He}$	$(-4.246 \pm 2.128) \times 10^1$	-0.522 ± 0.222	0	0	0	0
${}^7\mathrm{Li} + d \to n + {}^4\mathrm{He} + {}^4\mathrm{He}$	2.968×10^3	8.279	-0.308	0	54.611	0
${}^7\mathrm{Be} + d \to p + {}^4\mathrm{He} + {}^4\mathrm{He}$	$(5.817 \pm 0.843) \times 10^2$	0	0	0	-0.458 ± 0.010	0.057 ± 0.002

Table 10. Fit parameters according to eqs. (B.3), (B.10) and (B.11) for charged particle reactions. S_0 is given in MeV mb, a_k, q_k in $(\mathrm{MeV})^{-k}$.

and the non-relativistic ones like

$$\mathrm{bw}(E; k, \kappa, M) = \frac{k}{1 + \kappa(E - M)^2}, \tag{B.8}$$

with κ in $(\mathrm{MeV})^{-2}$ can be found in table 12 for the pertinent reactions.

For the function fits we use data composed by EXFOR [48, 49] for the cross section of 17 relevant reactions in BBN.

B.1 Radiative capture reactions

The parameters found by fitting data composed by [49] to eq. (B.3) are displayed in table 9 for most radiative capture reactions treated here. The parameterizations are compared to the corresponding data in figure 7.

The only exception is the reaction $\boldsymbol{d + {}^4\mathrm{He} \to {}^6\mathrm{Li} + \gamma}$, where a resonance appears. The S-factor here is given by

$$S(E) = S_0 \left(a_2 \cdot E^2 + \mathrm{BW}(E; 1, \Gamma, M) \right), \tag{B.9}$$

with the coefficients listed in tables 9 and 12.

B.2 Charged particle reactions

As in section B.1, we fit an S-factor like eq. (B.3). The parameters are listed in table 10 for the charged particle reactions treated here. The S-factor fits are displayed with the data composed by [49] in figures 8 and 9.

For the reactions $\boldsymbol{{}^6\mathrm{Li} + p \to {}^3\mathrm{He} + {}^4\mathrm{He}}$ and $\boldsymbol{{}^7\mathrm{Li} + p \to {}^4\mathrm{He} + {}^4\mathrm{He}}$ which have one (two) resonance(s), the S-factor is given by

$$S(E) = S_0 \left(1 + a_1 E + a_2 E^2 + a_3 E^3 + \mathrm{BW}(E; k_1, \Gamma_1, M_1) + \mathrm{BW}(E; k_2, \Gamma_2, M_2) \right). \tag{B.10}$$

JHEP06(2025)244

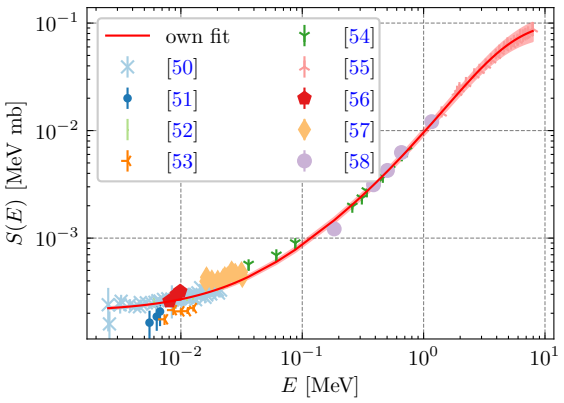

(a) $d + p \to {}^3\mathrm{He} + \gamma$

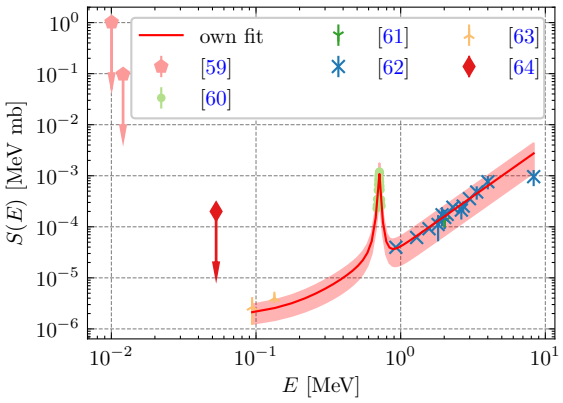

(b) $d + {}^4\mathrm{He} \to {}^6\mathrm{Li} + \gamma$

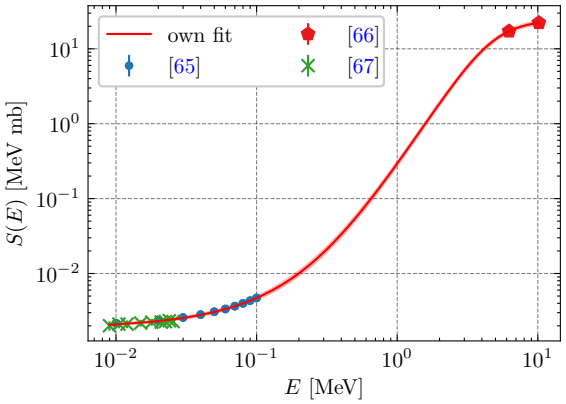

(c) ${}^3\mathrm{H} + p \to {}^4\mathrm{He} + \gamma$

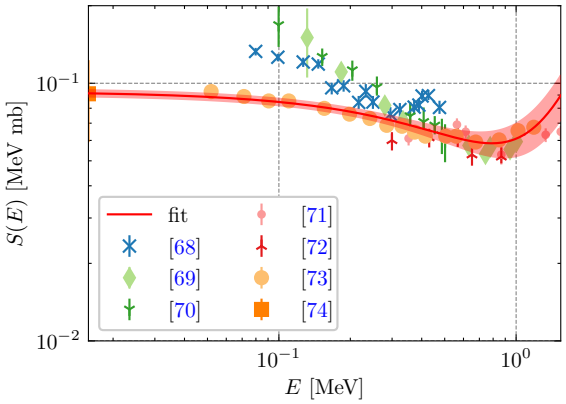

(d) ${}^3\mathrm{H} + {}^4\mathrm{He} \to {}^7\mathrm{Li} + \gamma$

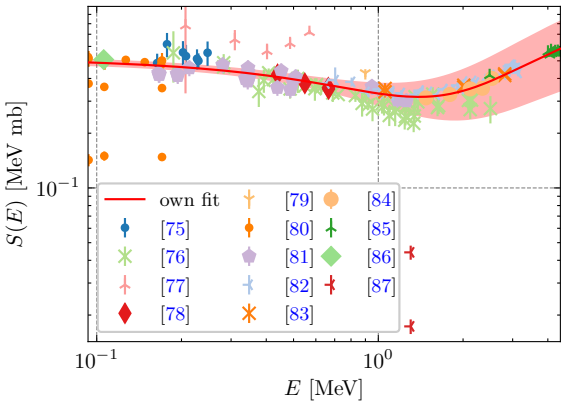

(e) ${}^3\mathrm{He} + {}^4\mathrm{He} \to {}^7\mathrm{Be} + \gamma$

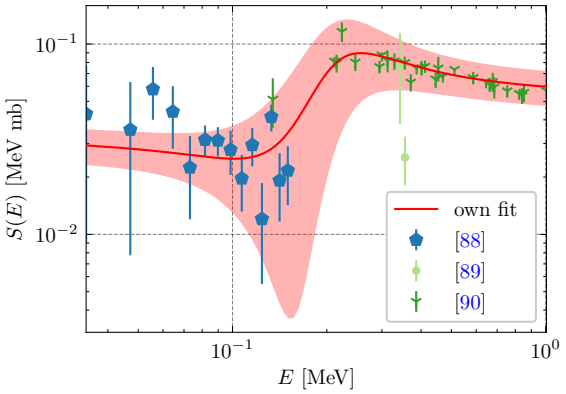

(f) ${}^6\mathrm{Li} + p \to {}^7\mathrm{Be} + \gamma$; error estimated using only ΔS_0 and Δa_1

Figure 7. Fits to experimental data composed by EXFOR [49] with error band for some relevant radiative capture reactions. The arrows on the data points in panel (b) indicate that these are upper bounds, not included in the fit.

JHEP06(2025)244

Reaction	$\mathcal{R}_0$	a_1	a_2	a_3	q_1	q_2	q_3
$^3\mathrm{He} + n \to p + {}^3\mathrm{H}$	$(7.053 \pm 0.034) \times 10^2$	8.359 ± 1.763	22.042 ± 2.556	1.571 ± 0.273	22.192 ± 2.708	-2.601 ± 2.445	6.462 ± 0.616
$^7\mathrm{Be} + n \to p + {}^7\mathrm{Li}$	$(6.962 \pm 0.035) \times 10^3$	9.375 ± 0.488	0	0	89.309 ± 3.542	0	0
$^7\mathrm{Be} + n \to {}^4\mathrm{He} + {}^4\mathrm{He}$	$(-2.765 \pm 1.01) \times 10^2$	-0.160 ± 0.010	0	0	0	0	0

Table 11. Fit parameters according to eq. (B.5) for neutron-induced reactions. $\mathcal{R}_0$ is given in $(\mathrm{MeV})^{1/2}\mathrm{mb}$, a_k, q_k in $(\mathrm{MeV})^{-k}$.

Reaction	k_1	Γ_1	M_1	k_2	Γ_2	M_2
$d + {}^4\mathrm{He} \to {}^6\mathrm{Li} + \gamma$	1	$.028 \pm 0.007$	$.711 \pm 0.002$			
$^6\mathrm{Li} + p \to {}^3\mathrm{He} + {}^4\mathrm{He}$	0.130 ± 0.088	0.397 ± 0.135	1.708 ± 0.042			
$^7\mathrm{Li} + p \to {}^4\mathrm{He} + {}^4\mathrm{He}$	-398.050 ± 189.573	0.866 ± 0.098	5.171 ± 0.032	-159.822 ± 64.838	0.872 ± 0.060	2.657 ± 0.017
$^7\mathrm{Be} + n \to p + {}^7\mathrm{Li}$	$(4.430 \pm 0.923) \times 10^{-4}$	0.162 ± 0.020	0.341 ± 0.006			
$^7\mathrm{Be} + n \to {}^4\mathrm{He} + {}^4\mathrm{He}$	-92.818 ± 35.910	3.644 ± 0.812	3.450 ± 0.118	-5.969 ± 2.532	3.253 ± 1.544	0.872 ± 0.218
	k_1	κ_1	M_1	k_2	κ_2	M_2
$^7\mathrm{Li} + d \to n + {}^4\mathrm{He} + {}^4\mathrm{He}$	9820.6	82.3871	0.6	8990.99	1963.84	0.8

Table 12. Fit parameters for resonances parameterized as Breit-Wigner functions (eq. (B.7) and eq. (B.8)). Γ_k, M_k are given in MeV, κ_k in $(\mathrm{MeV})^{-2}$. For the reaction $^7\mathrm{Li} + d \to n + {}^4\mathrm{He} + {}^4\mathrm{He}$ k is given in MeV mb, otherwise it is dimensionless.

For the reaction $\mathbf{^7Li + d \to n + {}^4He + {}^4He}$, we use the parameterization from [26] which has the form

$$S(E) = S_0 \frac{1 + a_1 E + a_2 E^2}{1 + q_1 E} + \mathrm{bw}(E; k_1, \kappa_1, M_1) + \mathrm{bw}(E; k_2, \kappa_2, M_2), \tag{B.11}$$

and estimate the error to be $\pm 97\%$ (so that almost all data points are included).

B.3 Neutron-induced reactions

The parameters found for three neutron-induced reactions parameterized here are displayed in table 11 and compared to data composed by [49] in figure 10.

The parameterization for the reactions $\mathbf{^7Be + n \to {}^7Li + p}$ (one resonance) and $\mathbf{^7Be + n \to {}^4He + {}^4He}$ (two resonances) is of the form

$$\mathcal{R}(E) = \mathcal{R}_0 \left(\frac{1 + a_1 E + a_2 E^2}{1 + q_1 E} + \mathrm{BW}(E; k_1, \Gamma_1, M_1) + \mathrm{BW}(E; k_2, \Gamma_2, M_2) \right). \tag{B.12}$$

JHEP06(2025)244

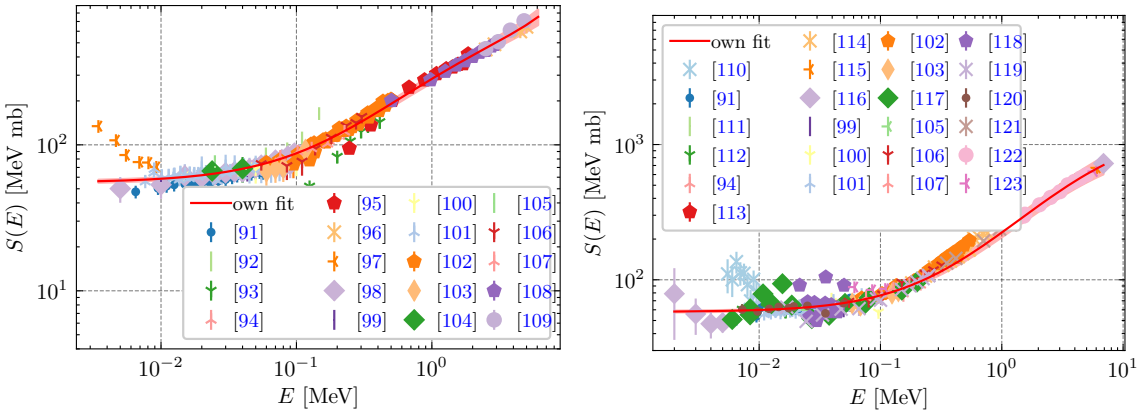

(a) $d + d \rightarrow {}^{3}\mathrm{He} + n$

(b) $d + d \rightarrow p + {}^{3}\mathrm{H}$

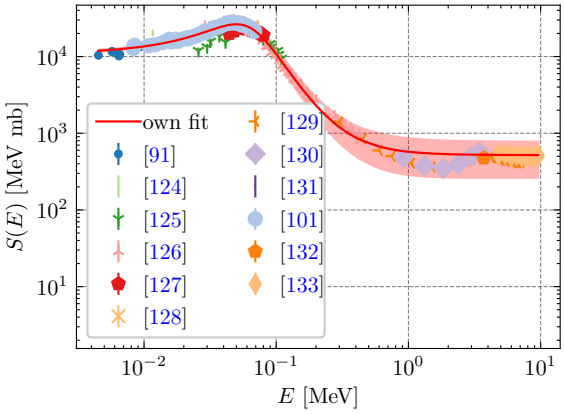

(c) ${}^{3}\mathrm{H} + d \rightarrow n + {}^{4}\mathrm{He}$

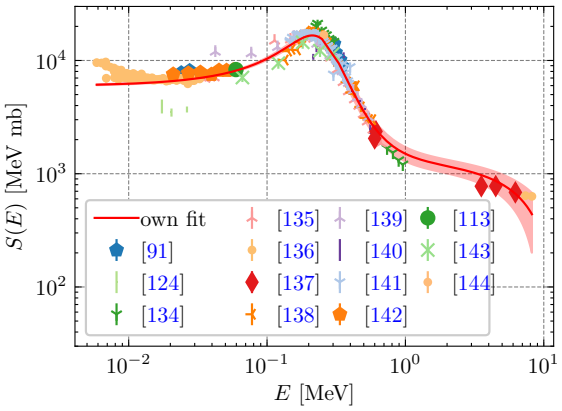

(d) ${}^{3}\mathrm{He} + d \rightarrow p + {}^{4}\mathrm{He}$

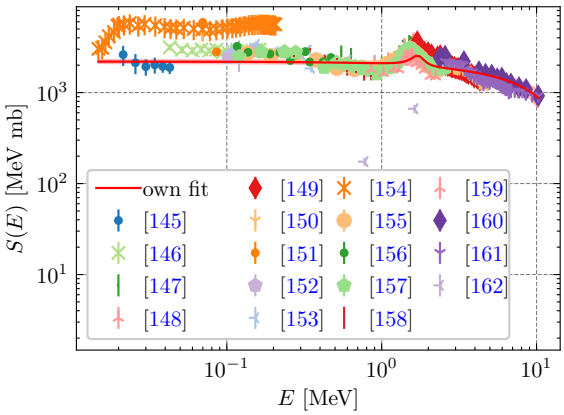

(e) ${}^{6}\mathrm{Li} + p \rightarrow {}^{3}\mathrm{He} + {}^{4}\mathrm{He}$

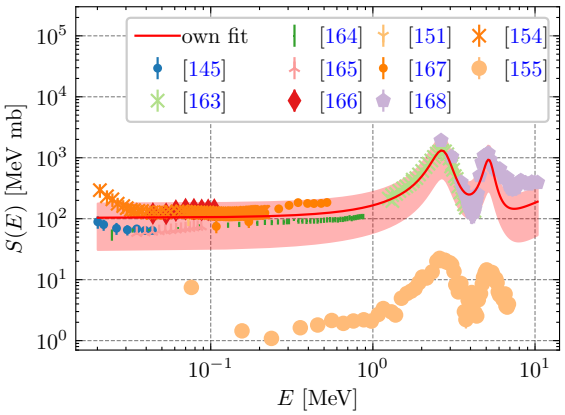

(f) ${}^{7}\mathrm{Li} + p \rightarrow {}^{4}\mathrm{He} + {}^{4}\mathrm{He}$

Figure 8. Fits to experimental data composed by EXFOR [49] with error bands for some relevant charged particle reactions.

JHEP06(2025)244

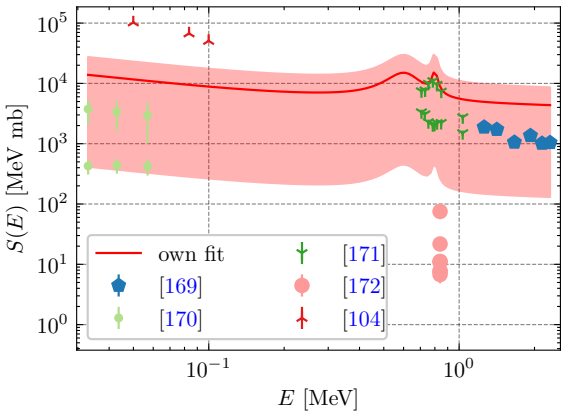

(a) $^{7}\mathrm{Li} + d \rightarrow n + {}^{4}\mathrm{He} + {}^{4}\mathrm{He}$; error estimated to ± 97.

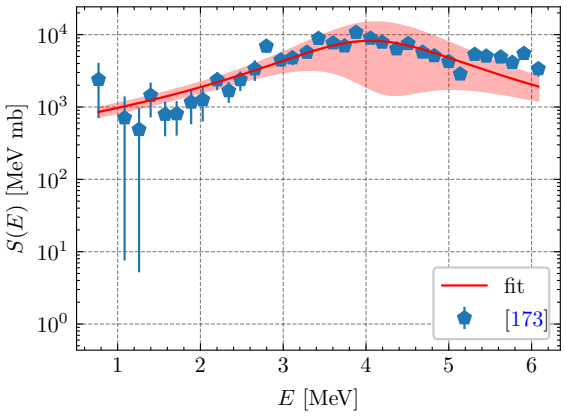

(b) $^{7}\mathrm{Be} + d \rightarrow p + {}^{4}\mathrm{He} + {}^{4}\mathrm{He}$

Figure 9. Fits to experimental data composed by EXFOR [49] with error bands for some relevant charged particle reactions with three particles in the final state.

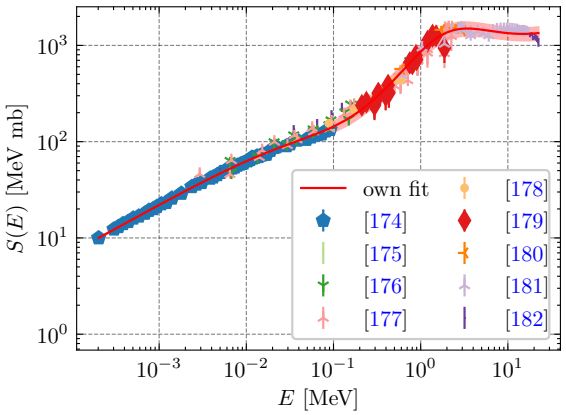

(a) $^{3}\mathrm{He} + n \rightarrow p + {}^{3}\mathrm{H}$

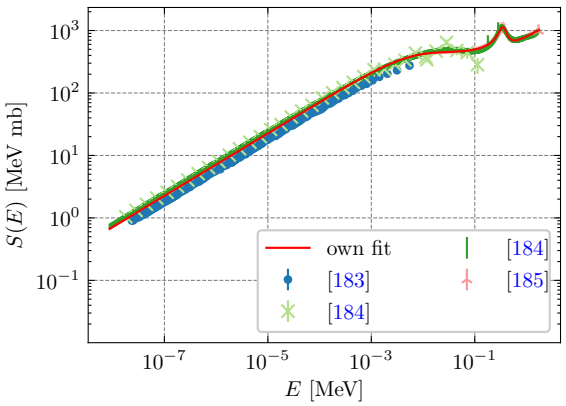

(b) $^{7}\mathrm{Be} + n \rightarrow p + {}^{7}\mathrm{Li}$

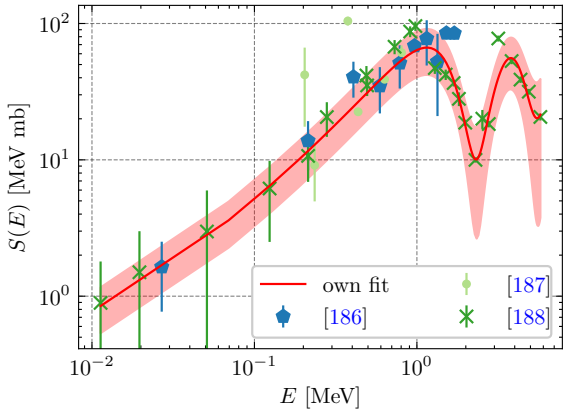

(c) $^{7}\mathrm{Be} + n \rightarrow {}^{4}\mathrm{He} + {}^{4}\mathrm{He}$; error estimated using only ΔS_0 and Δa_1.

Figure 10. Fits to experimental data composed by EXFOR [49] with error bands for some relevant neutron-induced reactions.

JHEP06(2025)244

Data Availability Statement. This article has no associated data or the data will not be deposited.

Code Availability Statement. This article has no associated code or the code will not be deposited.

Open Access. This article is distributed under the terms of the Creative Commons Attribution License (CC-BY4.0), which permits any use, distribution and reproduction in any medium, provided the original author(s) and source are credited.

References

[1] C.J. Hogan, *Why the universe is just so*, *Rev. Mod. Phys.* **72** (2000) 1149 [astro-ph/9909295] [INSPIRE].

[2] J.-P. Uzan, *The Fundamental Constants and Their Variation: Observational Status and Theoretical Motivations*, *Rev. Mod. Phys.* **75** (2003) 403 [hep-ph/0205340] [INSPIRE].

[3] A.N. Schellekens, *Life at the Interface of Particle Physics and String Theory*, *Rev. Mod. Phys.* **85** (2013) 1491 [arXiv:1306.5083] [INSPIRE].

[4] U.-G. Meißner, *Anthropic considerations in nuclear physics*, *Sci. Bull.* **60** (2015) 43 [arXiv:1409.2959] [INSPIRE].

[5] J.F. Donoghue, *The Multiverse and Particle Physics*, *Ann. Rev. Nucl. Part. Sci.* **66** (2016) 1 [arXiv:1601.05136] [INSPIRE].

[6] F.C. Adams, *The degree of fine-tuning in our universe — and others*, *Phys. Rept.* **807** (2019) 1 [arXiv:1902.03928] [INSPIRE].

[7] R.H. Cyburt, B.D. Fields, K.A. Olive and E. Skillman, *New BBN limits on physics beyond the standard model from* ^{4}He, *Astropart. Phys.* **23** (2005) 313 [astro-ph/0408033] [INSPIRE].

[8] M. Pospelov and J. Pradler, *Big Bang Nucleosynthesis as a Probe of New Physics*, *Ann. Rev. Nucl. Part. Sci.* **60** (2010) 539 [arXiv:1011.1054] [INSPIRE].

[9] F.K. Anagnostopoulos, V. Gakis, E.N. Saridakis and S. Basilakos, *New models and big bang nucleosynthesis constraints in f(Q) gravity*, *Eur. Phys. J. C* **83** (2023) 58 [arXiv:2205.11445] [INSPIRE].

[10] A.-K. Burns, T.M.P. Tait and M. Valli, *PRyMordial: the first three minutes, within and beyond the standard model*, *Eur. Phys. J. C* **84** (2024) 86 [arXiv:2307.07061] [INSPIRE].

[11] J.-P. Uzan, *Fundamental constants: from measurement to the universe, a window on gravitation and cosmology*, arXiv:2410.07281 [INSPIRE].

[12] U.-G. Meißner, B.C. Metsch and H. Meyer, *The electromagnetic fine-structure constant in primordial nucleosynthesis revisited*, *Eur. Phys. J. A* **59** (2023) 223 [arXiv:2305.15849] [INSPIRE].

[13] A.-K. Burns, V. Keus, M. Sher and T.M.P. Tait, *Constraints on variation of the weak scale from big bang nucleosynthesis*, *Phys. Rev. D* **109** (2024) 123506 [arXiv:2402.08626] [INSPIRE].

[14] H. Meyer and U.-G. Meißner, *Improved constraints on the variation of the weak scale from Big Bang nucleosynthesis*, *JHEP* **06** (2024) 074 [*Erratum ibid.* **01** (2025) 033] [arXiv:2403.09325] [INSPIRE].

JHEP06(2025)244

[15] F.E. Maas and K.D. Paschke, *Strange nucleon form-factors*, *Prog. Part. Nucl. Phys.* **95** (2017) 209 [INSPIRE].

[16] Flavour Lattice Averaging Group (FLAG) collaboration, *FLAG Review 2024*, arXiv:2411.04268 [INSPIRE].

[17] N. Kaiser, *Isospin breaking in neutron beta decay and $SU(3)$ violation in semileptonic hyperon decays*, *Phys. Rev. C* **64** (2001) 028201 [nucl-th/0105043] [INSPIRE].

[18] P. Jain et al., *Realistic Pseudoscalar Vector Chiral Lagrangian and Its Soliton Excitations*, *Phys. Rev. D* **37** (1988) 3252 [INSPIRE].

[19] E. Epelbaum, H.-W. Hammer and U.-G. Meissner, *Modern Theory of Nuclear Forces*, *Rev. Mod. Phys.* **81** (2009) 1773 [arXiv:0811.1338] [INSPIRE].

[20] J.C. Collins, A. Duncan and S.D. Joglekar, *Trace and Dilatation Anomalies in Gauge Theories*, *Phys. Rev. D* **16** (1977) 438 [INSPIRE].

[21] R.J. Crewther, *Nonperturbative evaluation of the anomalies in low-energy theorems*, *Phys. Rev. Lett.* **28** (1972) 1421 [INSPIRE].

[22] N.K. Nielsen, *The Energy Momentum Tensor in a Nonabelian Quark Gluon Theory*, *Nucl. Phys. B* **120** (1977) 212 [INSPIRE].

[23] J.A. Wheeler, *Geons*, *Phys. Rev.* **97** (1955) 511 [INSPIRE].

[24] F. Wilczek, *Mass without mass. I: Most of matter*, *Phys. Today* **52N11** (1999) 11 [INSPIRE].

[25] M. Hoferichter, J.R. de Elvira, B. Kubis and U.-G. Meißner, *On the role of isospin violation in the pion-nucleon σ-term*, *Phys. Lett. B* **843** (2023) 138001 [arXiv:2305.07045] [INSPIRE].

[26] U.-G. Meißner and B.C. Metsch, *Probing nuclear observables via primordial nucleosynthesis*, *Eur. Phys. J. A* **58** (2022) 212 [arXiv:2208.12600] [INSPIRE].

[27] J.-W. Chen and M.J. Savage, *$np \to d\gamma$ for big bang nucleosynthesis*, *Phys. Rev. C* **60** (1999) 065205 [nucl-th/9907042] [INSPIRE].

[28] G. Rupak, *Precision calculation of $np \to d\gamma$ cross-section for big bang nucleosynthesis*, *Nucl. Phys. A* **678** (2000) 405 [nucl-th/9911018] [INSPIRE].

[29] E. Epelbaum et al., *Viability of Carbon-Based Life as a Function of the Light Quark Mass*, *Phys. Rev. Lett.* **110** (2013) 112502 [arXiv:1212.4181] [INSPIRE].

[30] E. Epelbaum et al., *Dependence of the triple-alpha process on the fundamental constants of nature*, *Eur. Phys. J. A* **49** (2013) 82 [arXiv:1303.4856] [INSPIRE].

[31] S. Elhatisari et al., *Alpha-alpha scattering in the Multiverse*, *JHEP* **02** (2022) 001 [arXiv:2112.09409] [INSPIRE].

[32] N. Li et al., *Neutron-proton scattering with lattice chiral effective field theory at next-to-next-to-next-to-leading order*, *Phys. Rev. C* **98** (2018) 044002 [arXiv:1806.07994] [INSPIRE].

[33] L. Ubaldi, *Effects of theta on the deuteron binding energy and the triple-alpha process*, *Phys. Rev. D* **81** (2010) 025011 [arXiv:0811.1599] [INSPIRE].

[34] Particle Data Group collaboration, *Review of particle physics*, *Phys. Rev. D* **110** (2024) 030001 [INSPIRE].

[35] J.C. Berengut et al., *Varying the light quark mass: impact on the nuclear force and Big Bang nucleosynthesis*, *Phys. Rev. D* **87** (2013) 085018 [arXiv:1301.1738] [INSPIRE].

JHEP06(2025)244

[36] P.F. Bedaque, T. Luu and L. Platter, *Quark mass variation constraints from Big Bang nucleosynthesis*, *Phys. Rev. C* **83** (2011) 045803 [arXiv:1012.3840] [INSPIRE].

[37] S. Elhatisari et al., *Wavefunction matching for solving quantum many-body problems*, *Nature* **630** (2024) 59 [arXiv:2210.17488] [INSPIRE].

[38] T.A. Lähde and U.-G. Meißner, *Lattice Chiral Effective Field Theory: An introduction*, Springer International Publishing (2019) [DOI:10.1007/978-3-030-14189-9].

[39] P.D. Serpico et al., *Nuclear reaction network for primordial nucleosynthesis: A detailed analysis of rates, uncertainties and light nuclei yields*, *JCAP* **12** (2004) 010 [astro-ph/0408076] [INSPIRE].

[40] B.D. Fields, *The primordial lithium problem*, *Ann. Rev. Nucl. Part. Sci.* **61** (2011) 47 [arXiv:1203.3551] [INSPIRE].

[41] C. Pitrou, A. Coc, J.-P. Uzan and E. Vangioni, *Precision big bang nucleosynthesis with improved Helium-4 predictions*, *Phys. Rept.* **754** (2018) 1 [arXiv:1801.08023] [INSPIRE].

[42] L. Kawano, *Let's go: Early universe. 2. Primordial nucleosynthesis: The Computer way*, FERMILAB-PUB-92-004-A (1992) [INSPIRE].

[43] A. Arbey, *AlterBBN: A program for calculating the BBN abundances of the elements in alternative cosmologies*, *Comput. Phys. Commun.* **183** (2012) 1822 [arXiv:1106.1363] [INSPIRE].

[44] A. Arbey, J. Auffinger, K.P. Hickerson and E.S. Jenssen, *AlterBBN v2: A public code for calculating Big-Bang nucleosynthesis constraints in alternative cosmologies*, *Comput. Phys. Commun.* **248** (2020) 106982 [arXiv:1806.11095] [INSPIRE].

[45] Jülich Supercomputing Centre, *JURECA: Data Centric and Booster Modules implementing the Modular Supercomputing Architecture at Jülich Supercomputing Centre*, *JLSRF* **7** (2021) A182.

[46] J.J. de Swart, C.P.F. Terheggen and V.G.J. Stoks, *The Low-energy n p scattering parameters and the deuteron*, in the proceedings of the *3rd International Symposium on Dubna Deuteron 95*, Dubna, Russian Federation, July 04–07 (1995) [nucl-th/9509032] [INSPIRE].

[47] R. Machleidt, *The High precision, charge dependent Bonn nucleon-nucleon potential (CD-Bonn)*, *Phys. Rev. C* **63** (2001) 024001 [nucl-th/0006014] [INSPIRE].

[48] N. Otuka et al., *Towards a More Complete and Accurate Experimental Nuclear Reaction Data Library (EXFOR): International Collaboration Between Nuclear Reaction Data Centres (NRDC)*, *Nucl. Data Sheets* **120** (2014) 272 [arXiv:2002.07114] [INSPIRE].

[49] V.V. Zerkin and B. Pritychenko, *The Experimental Nuclear Reaction Data (EXFOR): Extended Computer Database and Web Retrieval System*, *Nucl. Instrum. Meth. Phys. Res. A* **888** (2018) 31 [arXiv:1802.05714].

[50] LUNA collaboration, *First measurement of the* $d(p,\gamma)^3$He *cross section down to the solar Gamow peak*, *Nucl. Phys. A* **706** (2002) 203 [INSPIRE].

[51] V.M. Bystritsky et al., *Using a hall accelerator to investigate* $d(d,n)^3$He *and* $d(p,\gamma)^3$He *reactions in the astrophysical energy region*, *Bull. Russ. Acad.* **74** (2010) 531.

[52] V.M. Bystritsky et al., *First experimental evidence of* $D(p,\gamma)^3$He *reaction in deuteride titanium in ultralow collision energy region*, *Nucl. Instrum. Meth. A* **753** (2014) 91 [INSPIRE].

[53] V.M. Bystritsky et al., *Study of the* $d(p,\gamma)^3$He *reaction at ultralow energies using a zirconium deuteride target*, *Nucl. Instrum. Meth. A* **737** (2014) 248 [arXiv:1306.6783] [INSPIRE].

JHEP06(2025)244

[54] G.M. Bailey et al., *Gamma-ray yields from the reaction* $d(p,\gamma)\,^3$He *at low energies*, Can. J. Phys. **48** (1970) 3059.

[55] W. Wölfli, R. Bösch and J. Lang, *Einfang von protonen durch deuteronen*, Helv. Phys. Acta **40** (1967) 946.

[56] V. Bystritsky et al., *Study of the pd reaction in the astrophysical energy region using the hall accelerator*, Nucl. Instrum. Meth. Phys. Res. A **595** (2008) 543.

[57] G.M. Griffiths, M. Lal and C.D. Scarfe, *The reaction* $d(p,\gamma)\,^3$He *below* 50 *keV*, Can. J. Phys. **41** (1963) 724.

[58] G.M. Griffiths, E.A. Larson and L.P. Robertson, *The capture of protons by deuterons*, Can. J. Phys. **40** (1962) 402.

[59] Y.B. Burkatovskaya et al., *Investigation of the reaction* $D(\,^4\mathrm{He},\gamma)\,^6$Li *at ultralow energies*, Phys. Part. Nucl. Lett. **13** (2016) 190 [INSPIRE].

[60] P. Mohr et al., *Direct capture in the* 3^+ *resonance of* $^2\mathrm{H}(\alpha,\gamma)\,^6$Li, Phys. Rev. C **50** (1994) 1543 [INSPIRE].

[61] J.C. Kim, *Radiative* α *particle capture in* ^{2}H *at* $e_\alpha = 6$ *MeV*, JKPS **15** (1982) 101.

[62] R.G.H. Robertson et al., *Observation of the capture reaction* $^2\mathrm{H}(\alpha,\,\gamma)\,^6$Li *and its role in production of* ^{6}Li *in the big bang*, Phys. Rev. Lett. **47** (1981) 1867 [*Erratum ibid.* **75** (1995) 4334] [INSPIRE].

[63] LUNA collaboration, *First Direct Measurement of the* $^2\mathrm{H}(\alpha,\gamma)\,^6$Li *Cross Section at Big Bang Energies and the Primordial Lithium Problem*, Phys. Rev. Lett. **113** (2014) 042501 [INSPIRE].

[64] F.E. Cecil, J. Yan and C.S. Galovich, *The reaction* $d(\alpha,\gamma)\,^6$Li *at low energies and the primordial nucleosynthesis of* ^{6}Li, Phys. Rev. C **53** (1996) 1967 [INSPIRE].

[65] R.S. Canon et al., $^3\mathrm{H}(p,\gamma)\,^4$He *reaction below* $E_p = 80$keV, Phys. Rev. C **65** (2002) 044008 [INSPIRE].

[66] J.R. Calarco et al., *Absolute cross section for the reaction* $^3\mathrm{H}(\mathrm{p},\gamma_0)\,^4$He *and a review of* $^4\mathrm{He}(\gamma,\mathrm{p}_0)\,^3$H *measurements*, Phys. Rev. C **28** (1983) 483 [INSPIRE].

[67] V.A. Varlachev et al., *Measurement of the S-Factor of the* $\mathrm{T}(\,^1\mathrm{H},\gamma)\,^4$He *Reaction at Astrophysical Energies*, JETP Lett. **113** (2021) 231 [INSPIRE].

[68] U. Schröder et al., *Astrophysical S-factor of* $^3\mathrm{H}(\alpha,\gamma)\,^7$Li, Phys. Lett. B **192** (1987) 55 [INSPIRE].

[69] H. Utsunomiya et al., *Breakup of* ^{7}Li *near the* α-t *threshold and a possible probe of radiative-capture processes*, Phys. Rev. Lett. **65** (1990) 847 [INSPIRE].

[70] Y. Tokimoto et al., *Coulomb breakup of* ^{7}Li *for nuclear astrophysics*, Phys. Rev. C **63** (2001) 035801 [INSPIRE].

[71] G.M. Griffiths et al., *The* $t(\alpha,\gamma)\,^7$Li *reaction*, Can. J. Phys. **39** (1961) 1397.

[72] S. Burzyński, K. Czerski, A. Marcinkowski and P. Zupranski, *The* $^3\mathrm{H}(\alpha,\gamma)\,^7$Li *reaction in the energy range from 0.7 to 2.0 MeV*, Nucl. Phys. A **473** (1987) 179 [INSPIRE].

[73] C.R. Brune, R.W. Kavanagh and C. Rolfs, *H-3 (alpha, gamma) Li-7 reaction at low energies*, Phys. Rev. C **50** (1994) 2205 [INSPIRE].

[74] V.M. Bystritsky et al., *Astrophysical S-factor of* $T(\,^4\mathrm{He},\gamma)\,^7$Li *reaction at* $E_{cm} = 15.7$ *keV*, Phys. Part. Nucl. Lett. **14** (2017) 560 [INSPIRE].

JHEP06(2025)244

[75] K. Nagatani, M.R. Dwarakanath and D. Ashery, *The $^{3}He(\alpha,\gamma)\,^{7}Be$ reaction at very low energy*, *Nucl. Phys. A* **128** (1969) 325 [INSPIRE].

[76] P.D. Parker and R.W. Kavanagh, $he^{3}(\alpha,\gamma)be^{7}$ *reaction*, *Phys. Rev.* **131** (1963) 2578 [INSPIRE].

[77] H.D. Holmgren and R.L. Johnston, $h^{3}(\alpha,\gamma)li^{7}$ *and* $he^{3}(\alpha,\gamma)be^{7}$ *reactions*, *Phys. Rev.* **113** (1959) 1556 [INSPIRE].

[78] M. Hilgemeier et al., *Absolute cross section of the* $^{3}\mathrm{He}(\alpha,\gamma)\,^{7}\mathrm{Be}$ *reaction*, *Z. Phys. A* **329** (1988) 243.

[79] R.G.H. Robertson et al., *Cross section of the capture reaction* $^{3}\mathrm{He}(\alpha,\gamma)\,^{7}\mathrm{Be}$, *Phys. Rev. C* **27** (1983) 11 [INSPIRE].

[80] H. Costantini et al., *The* $^{3}\mathrm{He}(\alpha,\gamma)\,^{7}\mathrm{Be}S$*-factor at solar energies: The Prompt gamma experiment at LUNA*, *Nucl. Phys. A* **814** (2008) 144 [arXiv:0809.5269] [INSPIRE].

[81] J.L. Osborne et al., *Low-energy Behavior of the* $^{3}\mathrm{He}(\alpha,\gamma)\,^{7}\mathrm{Be}$ *Cross-section*, *Nucl. Phys. A* **419** (1984) 115 [INSPIRE].

[82] A. Di Leva et al., *Stellar and primordial nucleosynthesis of* ^{7}*Be: Measurement of* $^{3}\mathrm{He}(\alpha,\gamma)\,^{7}\mathrm{Be}$, *Phys. Rev. Lett.* **102** (2009) 232502 [*Erratum ibid.* **103** (2009) 159903] [INSPIRE].

[83] M. Carmona-Gallardo et al., *New measurement of the* $^{3}\mathrm{He}(\alpha,\gamma)\,^{7}\mathrm{Be}$ *cross section at medium energies*, *Phys. Rev. C* **86** (2012) 032801 [INSPIRE].

[84] C. Bordeanu et al., *Activation measurement of the* $^{3}\mathrm{He}(\alpha,\gamma)\,^{7}\mathrm{Be}$ *reaction cross section at high energies*, *Nucl. Phys. A* **908** (2013) 1 [arXiv:1304.4740] [INSPIRE].

[85] T. Szücs et al., *Cross section of* $^{3}He(\alpha,\gamma)\,^{7}Be$ *around the* ^{7}*Be proton separation threshold*, *Phys. Rev. C* **99** (2019) 055804 [*Erratum ibid.* **105** (2022) 069901] [arXiv:1905.01711] [INSPIRE].

[86] G. Gyürky et al., $^{3}\mathrm{He}(\alpha,\gamma)\,^{7}\mathrm{Be}$ *cross section at low energies*, *Phys. Rev. C* **75** (2007) 035805 [nucl-ex/0702003] [INSPIRE].

[87] T.K. Alexander et al., *Measurement of the absolute cross section of the* $^{3}\mathrm{He}(\,^{4}\mathrm{He},\gamma)\,^{7}\mathrm{Be}$ *reaction at* $E_{\mathrm{c.m.}} = 525\,keV$, *Nucl. Phys. A* **427** (1984) 526 [INSPIRE].

[88] R. Bruss et al., *Astrophysical s-factors for the radiative capture reaction* $^{6}\mathrm{Li}(p,\gamma_1)\,^{7}\mathrm{Be}^{*}$ *at low energies*, in *Nuclei in the Cosmos*, CRC Press, Karlsruhe (1992) [DOI:10.1201/9781003062974].

[89] S. Bashkin and R.R. Carlson, *Gamma rays from proton bombardment of* li^{6}, *Phys. Rev.* **97** (1955) 1245.

[90] Z.E. Switkowski et al., *Cross section of the reaction* $^{6}Li(p,\gamma)\,^{7}Be$, *Nucl. Phys. A* **331** (1979) 50 [INSPIRE].

[91] W.R. Arnold et al., *Cross sections for the reactions* $\mathrm{D}(d,p)\mathrm{T}$, $\mathrm{D}(d,n)\mathrm{He}^{3}$, $\mathrm{T}(d,n)\mathrm{he}^{4}$, *and* $\mathrm{He}^{3}(d,p)\mathrm{he}^{4}$ *below 120 keV*, *Phys. Rev.* **93** (1954) 483 [INSPIRE].

[92] J.H. Manley et al., *Elastic backscattering of d-d neutrons*, *Phys. Rev.* **70** (1946) 602.

[93] P.R. Chagnon and G.E. Owen, *Angular distributions of the d+d neutrons*, *Phys. Rev.* **101** (1956) 1798.

[94] N. Ying, B.B. Cox, B.K. Barnes and A.W. Barrows, *A study of the* $^{2}\mathrm{H}(d,p)\,^{3}\mathrm{H}$ *and* $^{2}\mathrm{H}(d,n)\,^{3}\mathrm{He}$ *reactions and the excited state of* ^{4}He *at* 23.9 *MeV*, *Nucl. Phys. A* **206** (1973) 481 [INSPIRE].

[95] G.T. Hunter and H.T. Richards, *Yield and angular distribution of the d-d neutrons*, *Phys. Rev.* **76** (1949) 1445.

JHEP06(2025)244

[96] S.T. Thornton, *The $D(d,n)^3$He reaction from $E_d = 5$ to 10 MeV*, *Nucl. Phys. A* **136** (1969) 25 [INSPIRE].

[97] A.S. Belov, V.E. Kusik and Y.V. Ryabov, *The nuclear fusion for the reactions ^{2}H$(d,n)^3$He, ^{2}H$(d,\gamma)^4$He at low deuterons energy and "cold" nuclear fusion*, *Nuovo Cim. A* **103** (1990) 1647.

[98] V.A. Davidenko et al., *Total cross section measurement of $d(d,n)^3$He reaction in energy range 20 to 220 keV*, *Atomnaya Energiya* (1957) 7 [*Sov. J. Atomic Energy (English Translation)* **Suppl. 5** (1958)].

[99] R.E. Brown and N. Jarmie, *Differential cross sections at low energies for ^{2}H$(d,p)^3h$ and ^{2}H$(d,n)^3he$*, *Phys. Rev. C* **41** (1990) 1391 [INSPIRE].

[100] U. Greife et al., *Oppenheimer-phillips effect and electron screening in $d+d$ fusion reactions*, *Z. Phys. A* **351** (1995) 107.

[101] T.F.R. Group and T.F.R. Division, *Low energy cross-sections measurement of d-d and d-t reactions*, *High. Energ. Phys. Nuc* **9** (1985) 723.

[102] A.S. Ganeev et al., *The d-d reaction in the deuteron energy range 100–1000 keV*, *Atomnaya Energiya* (1957) 26 [*Soviet J. Atomic Energy (English Translation)* **Suppl. 5** (1958)].

[103] K.G. McNeill and G.M. Keyser, *The relative probabilities and absolute cross sections of the $d-d$ reactions*, *Phys. Rev.* **81** (1951) 602.

[104] M.A. Hofstee et al., *Measurement of low energy (d,n) reactions on light nuclei important to astrophysics*, *Nucl. Phys. A* **688** (2001) 527 [INSPIRE].

[105] D.L. Booth, G. Preston and P.F.D. Shaw, *The cross section and angular distributions of the d-d reactions between 40 and 90 keV*, *Proc. Phys. Soc. A* **69** (1956) 265.

[106] D.S. Leonard et al., *Precision measurements of ^{2}H$(d,p)^3$H and ^{2}H$(d,n)^3$He total cross sections at big bang nucleosynthesis energies*, *Phys. Rev. C* **73** (2006) 045801 [INSPIRE].

[107] G. Preston et al., *The cross-sections and angular distributions of the d-d reactions between* 150 *and* 450 *KeV*, *Proc. Roy. Soc. Lond. A* **226** (1954) 206.

[108] R.L. Schulte, M. Cosack, A.W. Obst and J.L. Weil, *^{2}H+ reactions from 1.96 to 6.20 MeV*, *Nucl. Phys. A* **192** (1972) 609 [INSPIRE].

[109] M.D. Goldberg and J.M. Le Blanc, *Angular distributions of the* D$(d,n)^3$He *reaction for* 5- *to* 12 *MeV deuterons*, *Phys. Rev.* **119** (1960) 1992.

[110] W. Tie-Shan et al., *Measurement of d(d,p)t reaction cross sections in sm metal in low energy region ($10 \leq e_d \leq 20$ keV)*, *Chin. Phys. Lett.* **24** (2007) 3103.

[111] J.H. Sanders, J. Moffat and D. Roaf, *The low energy cross section and angular distribution of the d(d,p) reaction*, *Phys. Rev.* **77** (1950) 754.

[112] J. Moffatt et al., *The $D-D$ cross-section and angular distribution below 50 keV*, *Proc. Roy. Soc. Lond. A* **212** (1952) 220.

[113] A. Krauss et al., *Low-energy fusion cross sections of $D+D$ and $D+^3$He reactions*, *Nucl. Phys. A* **465** (1987) 150 [INSPIRE].

[114] V.V. Volkov et al., *Investigation of the d-d reaction in the deuteron energy range* 0.20 *to* 1.75 *MeV*, *Atomnaya Energiya* (1957) 15.

[115] J.E. Brolley, T.M. Putnam and L. Rosen, *d-D Reactions at 6- to 14-MeV Input Energy*, *Phys. Rev.* **107** (1957) 820 [INSPIRE].

JHEP06(2025)244

[116] A. von Engel, C.C. Goodyear and B. Bleaney, *Fusion cross-section measurements with deuterons of low energy*, *Proc. Roy. Soc. Lond. A* **264** (1961) 445.

[117] P.A. Davenport et al., *The $d-d$ cross-section and angular distribution between 55 and 430 keV*, *Proc. Roy. Soc. Lond. A* **216** (1953) 66.

[118] C.F. Cook and J.R. Smith, *Cross section for the reaction* $\mathrm{D}(d,p)\mathrm{h}^3$, *Phys. Rev.* **89** (1953) 785.

[119] W.A. Wenzel and W. Whaling, *Cross section and angular distribution of the* $\mathrm{D}(d,p)\mathrm{T}$ *reaction*, *Phys. Rev.* **88** (1952) 1149.

[120] E. Bretscher, A.P. French and F.G.P. Seidl, *Low energy yield of* $\mathrm{D}(\mathrm{D},p)\mathrm{H}^3$ *and the angular distribution of the emitted protons*, *Phys. Rev.* **73** (1948) 815.

[121] W. Grüebler et al., *New highly excited* ^{4}He *levels found by the* $^2\mathrm{H}(d,p)\,^3\mathrm{H}$ *reaction*, *Nucl. Phys. A* **369** (1981) 381 [INSPIRE].

[122] W. Grüebler et al., *Investigation of excited states of* ^{4}He *via the* $^2\mathrm{H}(d,p)\,^3\mathrm{H}$ *and* $^2\mathrm{H}(d,n)\,^3$He *reactions using a polarized deuteron beam*, *Nucl. Phys. A* **193** (1972) 129 [INSPIRE].

[123] A.C. Graves et al., *Cross section of* $d(d,p)\,^3\mathrm{H}$ *reaction*, *Phys. Rev.* **70** (1946) 101.

[124] R.G. Jarvis, D. Roaf and L. Cherwell, *Comparison of d-t and d-*^{3}He *at low energies*, *Proc. Roy. Soc. Lond. A* **218** (1953) 432.

[125] V.A. Davidenko, I.S. Poerebou and A.I. Saukov, *The shape of the excitation curve for the* $t(d,n)\,^4$He *reaction*, *Atomnaya Energiya* **2** (1957) 386.

[126] E.M. Balabanov et al., *Effective cross section measurement of* $d(t,n)\,^4$He *reaction in deuteron energy range 40 to 730 keV*, *Atomnaya Energiya* **Suppl. 5** (1957) 57.

[127] D.L. Allan, M.J. Poole and J.D. Cockcroft, *Experiments on the reaction* $t(d,n)\,^4he$ *I. The* 90° *cross-section*, *Proc. Roy. Soc. Lond. A* **204** (1951) 488.

[128] J.P. Conner, T.W. Bonner and J.R. Smith, *A study of the* $\mathrm{h}^3(d,n)\mathrm{he}^4$ *reaction*, *Phys. Rev.* **88** (1952) 468.

[129] S.J. Bame and J.E. Perry, $\mathrm{T}(d,n)\mathrm{he}^4$ *reaction*, *Phys. Rev.* **107** (1957) 1616.

[130] A. Galonsky and C.H. Johnson, *Cross sections for the* $\mathrm{T}(d,n)\mathrm{he}^4$ *reaction*, *Phys. Rev.* **104** (1956) 421.

[131] R.E. Brown, N. Jarmie and G.M. Hale, *Fusion-energy reaction* $^3H(d,\alpha)n$ *at low energies*, *Phys. Rev. C* **35** (1987) 1999 [INSPIRE].

[132] M.D. Goldberg and J.M. Le Blanc, *Angular yield of neutrons from the* $\mathrm{T}(d,n)\mathrm{He}^4$ *reaction for 6- to 11.5-MeV deuterons*, *Phys. Rev.* **122** (1961) 164.

[133] E. Magiera, M. Bormann, W. Scobel and P. Heiss, *Angular distributions of neutrons from the 3 H(d, n) 4 He reaction*, *Nucl. Phys. A* **246** (1975) 413 [INSPIRE].

[134] G. Freier and H. Holmgren, *Interaction between D-2 and He-3 in the Neighborhood of the 18.6-MeV Level of Li-5*, *Phys. Rev.* **93** (1954) 825 [INSPIRE].

[135] T.W. Bonner, J.P. Conner and A.B. Lillie, *Cross section and angular distribution of the* $\mathrm{he}^3(d,p)\mathrm{he}^4$ *nuclear reaction*, *Phys. Rev.* **88** (1952) 473.

[136] S. Engstler et al., *Effects of electron screening on the 3 He(d, p) 4 He low-energy cross sections*, *Phys. Lett. B* **202** (1988) 179 [INSPIRE].

[137] L. Stewart, J.E. Brolley and L. Rosen, *Interaction of 6- to 14-MeV deuterons with helium three and tritium*, *Phys. Rev.* **119** (1960) 1649.

JHEP06(2025)244

[138] L. Zhichang, Y. Jingang and D. Xunliang, *Measurement of* ^{3}He$(d,p)^{4}$He *reaction cross sections*, *Atomic Energ. Sci. Technol.* **11** (1977) 229.

[139] M. La Cognata et al., *Bare-nucleus astrophysical factor of the* ^{3}He$(d,p)^{4}$He *reaction via the "trojan horse" method*, *Phys. Rev. C* **72** (2005) 065802 [INSPIRE].

[140] H. Erramli et al., *Measurements of the* ^{3}He$(d,p)^{4}$He *nuclear reaction cross section by coincidence detection of alphas and protons: Application to the determination of the* ^{3}He *desorption rate from helium bubbles in silicon*, *Phys. Chem. News* **23** (2005) 67.

[141] W.H. Geist et al., *The* ^{3}He$(d,p)^{4}$He *reaction at low energies*, *Phys. Rev. C* **60** (1999) 054003 [*Erratum ibid.* **67** (2003) 059904] [INSPIRE].

[142] J.L. Tuck et al., ^{3}He *d cross sections 35–100 keV*, *Phys. Rev.* **88** (1952) 159.

[143] D.L. Booth et al., *The reaction* ^{3}He$(d,p)^{4}$He *between 100 keV and 500 keV*, *Proc. Phys. Soc. A* **70** (1957) 863.

[144] J.L. Yarnell, R.H. Lovberg and W.R. Stratton, *Angular distribution of the reaction* He$^{3}(d,p)$He^{4} *between 240 keV and 3.56 MeV*, *Phys. Rev.* **90** (1953) 292.

[145] O. Fiedler and P. Kunze, *Wirkungsquerschnitte der Kernreaktionen* ^{6}Li$(p,\alpha)^{3}$He *und* ^{7}Li$(p,\alpha)^{4}$He *bei kleinsten Energien*, *Nucl. Phys. A* **96** (1967) 513 [INSPIRE].

[146] W. Gemeinhardt and D. Kamke and C. von Rhöneck, *Winkelverteilung und wirkungsquerschnitt der reaktion* ^{6}Li$(p,\alpha)^{3}$He *im energiebereich von 50 bis 190 keV*, *Z. Phys.* **197** (1966) 58.

[147] J.B. Marion, G. Weber and F.S. Mozer, *Study of the* li$^{6}(p,\alpha)$he^{3} *reaction*, *Phys. Rev.* **104** (1956) 1402 [INSPIRE].

[148] B.W. Hooton and M. Ivanovich, *The* ^{6}Li$(p,\,^{3}$He$)^{4}$He *reaction*, tech. rep., Prog: A.E.R.E Harwell Reports, (1972).

[149] J.M.F. Jeronymo, G.S. Mani and A. Sadeghi, *The* ^{6}Li$(p,\alpha)^{3}$He *reaction*, *Nucl. Phys.* **43** (1963) 424.

[150] U. Fasoli, D. Toniolo and G. Zago, *The* ^{6}Li$(p,\,^{3}$He$)^{4}$He *reaction in the energy range* 3–5.6 *MeV*, *Phys. Lett.* **8** (1964) 127.

[151] LUNA collaboration, *Electron screening in* ^{7}Li$(p,\alpha)\alpha$ *and* ^{6}Li$(p,\alpha)^{3}$He *for different environments*, *Phys. Lett. B* **624** (2005) 181 [INSPIRE].

[152] M. Várnagy et al., *Application of t-cellit detector for the study of* ^{6,7}Li$(p,\alpha)^{3,4}$He *reactions*, *Nucl. Instrum. Meth.* **119** (1974) 451.

[153] T. Shinozuka, Y. Tanaka and K. Sugiyama, *Absolute cross sections for the* ^{6}Li$(p,\,^{3}$He$)^{4}$He *reaction at energies below 1 MeV*, *Nucl. Phys. A* **326** (1979) 47 [INSPIRE].

[154] G.A. Sawyer and J.A. Phillips, *Charged particle cross sections*, tech. rep., Los Alamos Scientific Lab. Reports, (1953).

[155] A. Tumino et al., *Validity test of the "Trojan horse" method applied to the* ^{6}Li$(p,\alpha)^{3}$He *reaction*, *Phys. Rev. C* **67** (2003) 065803 [INSPIRE].

[156] J.U. Kwon, J.C. Kim and B.N. Sung, *Low-energy cross sections for the* ^{6}Li$(p,\,^{3}$He$)^{4}$He *reaction*, *Nucl. Phys. A* **493** (1989) 112 [INSPIRE].

[157] A.J. Elwyn et al., *Cross sections for the* ^{6}Li$(p,\,^{3}$He$)^{4}$He *reaction at energies between* 0.1 *and* 3.0 *MeV*, *Phys. Rev. C* **20** (1979) 1984 [INSPIRE].

JHEP06(2025)244

[158] F. Bertrand, G. Grenier and J. Pornet, ^{6}Li$(p,\alpha)\,^{3}$He, ^{6}Li$(d,\alpha)\,^{4}$He, ^{6}Li$(d0)\,^{7}$Li, ^{6}Li$(d1)\,^{7}$Li* *reaction investigation in the energy interval from 300 keV to 1000 keV*, tech. rep., Centre d'Etudes Nucleaires, Saclay (1968).

[159] L. Chia-Shou, H. Wan-Shou, W. Min and C. Jen-Chang, *Cross-section measurements for the* ^{6}Li$(p,\alpha)\,^{3}$He *reaction in the proton energy range* $1.0-2.6$ *MeV*, *Nucl. Phys. A* **275** (1977) 93 [INSPIRE].

[160] G.M. Temmer, *Detailed* (p,α) *reaction studies on the lighter nuclei with the florida state university tandem accelerator*, in the proceedings of the *Conference on Direct Interactions and Nuclear. Reaction Mechanisms*, Padua, September 3–8 (1962), p. 1013.

[161] C.R. Gould et al., *Cross-section requirements for charged-particle fusion reactors: The* ^{6}Li$(p,\,^{3}$He$)\alpha$ *reaction*, *Nucl. Sci. Eng.* **55** (1974) 267.

[162] H. Spinka, T. Tombrello and H. Winkler, *Low-energy cross sections for* ^{7}Li$(p,\alpha)\,^{4}$He *and* ^{6}Li$(p,\alpha)\,^{3}$He, *Nucl. Phys. A* **164** (1971) 1 [INSPIRE].

[163] Y. Cassagnou et al., *The* ^{7}Li$(p,\alpha)\alpha$ *reaction*, *Nucl. Phys.* **33** (1962) 449.

[164] C. Rolfs and R.W. Kavanagh, *The* ^{7}Li$(p,\alpha)\,^{4}$He *cross section at low energies*, *Nucl. Phys. A* **455** (1986) 179 [INSPIRE].

[165] M. Spraker et al., *Slope of the astrophysical s factor for the* ^{7}Li$(p,\gamma)\,^{8}$Be *reaction*, *Phys. Rev. C* **61** (2000) 015802 [INSPIRE].

[166] C.C. Lee, *A study on the* ^{7}Li $+\,p$ *and* ^{6}Li $+\,d$ *nuclear reactions*, *JKPS* **2** (1969) 1.

[167] D.M. Ciric et al., *The interaction of* ^{7}Li *isotope with low energy proton and triton beams*, *Rev. Res.* **6** (1976) 115.

[168] G.S. Mani et al., *Study of the reaction* ^{7}Li$(p,\alpha)\alpha$ *up to 12 MeV proton energy*, *Nucl. Phys.* **60** (1964) 588.

[169] G.M. Osetinskii et al., *Investigation of the reaction* ^{7}Li$(d,n)\,^{8}$Be, tech. rep., Joint. Inst. for Nucl. Res., Dubna (1970).

[170] A. Sabourov et al., *Astrophysical s factor for the* ^{7}Li$(d,n_0)\,^{8}$Be *and* ^{7}Li$(d,n_1)\,^{8}$Be *reactions*, *Phys. Rev. C* **73** (2006) 015801 [INSPIRE].

[171] C. Nussbaum, *Effects of the interference in the reactions* ^{7}Li$(d,n)\,^{8}$Be *near 1 MeV resonance*, *Helv. Phys. Acta* **42** (1969) 361.

[172] J. Catalá et al., *Distribuciones angulares de los neutrones producidos en la reacción* ^{7}Li$(d,n)\,^{8}$Be, *Nuovo Cim.* **9** (1958) 377.

[173] N. Rijal et al., *Measurement of* $d+\,^{7}$*Be cross sections for Big-Bang nucleosynthesis*, *Phys. Rev. Lett.* **122** (2019) 182701 [*Erratum ibid.* **123** (2019) 239902] [arXiv:1808.07893] [INSPIRE].

[174] S.B. Borzakov et al., *Peculiarities in deviation from the* v^{-1} *law for* ^{3}He$(n,p)t$ *reaction cross section. excited level of the* ^{4}He *nucleus*, *Yad. Fiz.* **35** (1982) 532.

[175] D.G. Costello, S.J. Friesenhahn and W.M. Lopez, ^{3}He$(n,p)t$ *cross section from* 0.3 *to* 1.16 *MeV*, *Nucl. Sci. Eng.* **39** (1970) 409.

[176] R.L. Macklin and J.H. Gibbons, *On the absolute value and energy dependence of the* ^{3}He(n,p) *reaction*, in the proceedings of the *International Conference on the Study of Nuclear Structure with Neutrons* Antwerp, Belgium, July 19–23 (1965).

[177] J.H. Gibbons and R.L. Macklin, *Total Neutron Yields from Light Elements under Proton and Alpha Bombardment*, *Phys. Rev.* **114** (1959) 571 [INSPIRE].

JHEP06(2025)244

[178] R. Batchelor, R. Aves and T.H.R. Skyrme, *Helium-3 filled proportional counter for neutron spectroscopy*, *Rev. Sci. Instrum.* **26** (1955) 1037.

[179] J.H. Coon, *Disintegration of* He^3 *by fast neutrons*, *Phys. Rev.* **80** (1950) 488.

[180] A.R. Sayres, K.W. Jones and C.S. Wu, *Interaction of neutrons with* He^3, *Phys. Rev.* **122** (1961) 1853.

[181] B. Haesner et al., *Measurement of the* ^{3}He *and* ^{4}He *total neutron cross sections up to 40 MeV*, *Phys. Rev. C* **28** (1983) 995 [INSPIRE].

[182] R.G. Pizzone et al., *Indirect measurement of the* $^3He(n,p)^3H$ *reaction cross section at Big Bang energies*, *Eur. Phys. J. A* **56** (2020) 199 [INSPIRE].

[183] P.E. Koehler et al., *Be-7 (n, p) Li-7 total cross section from 25 MeV to 13.5 keV*, *Phys. Rev. C* **37** (1988) 917 [INSPIRE].

[184] n_TOF collaboration, $^7Be(n,p)^7Li$ *Reaction and the Cosmological Lithium Problem: Measurement of the Cross Section in a Wide Energy Range at n_TOF at CERN*, *Phys. Rev. Lett.* **121** (2018) 042701 [arXiv:1803.05701] [INSPIRE].

[185] J. Červená et al., *Investigation of* $^7\mathrm{Be}(n,p)^7\mathrm{Li}$ *reaction*, *Czech. J. Phys.* **39** (1989) 1263.

[186] L. Lamia et al., *Cross-section measurement of the cosmologically relevant* $^7\mathrm{Be}(n,\alpha)^4\mathrm{He}$ *reaction over a broad energy range in a single experiment*, *Astrophys. J.* **879** (2019) 23 [INSPIRE].

[187] T. Kawabata et al., *Time-reversal measurement of the p-wave cross sections of the* $^7\mathrm{Be}(n,\alpha)^4\mathrm{He}$ *reaction for the cosmological li problem*, *Phys. Rev. Lett.* **118** (2017) 052701 [INSPIRE].

[188] S.Q. Hou, J.J. He, S. Kubono and Y.S. Chen, *Revised thermonuclear rate of* $^7\mathrm{Be}(n,\alpha)^4\mathrm{He}$ *relevant to big-bang nucleosynthesis*, *Phys. Rev. C* **91** (2015) 055802 [arXiv:1502.03961] [INSPIRE].